IMAGE PROCESSING BASED APPROACH TO DETERMINE THE ANGLE OF INCIDENCE FOR BULLET HOLES, IN AID OF SHOOTING INCIDENT RECONSTRUCTION

W. R. C. Ariyarathna

2023

Image Processing Based Approach to Determine the Angle of Incidence for Bullet Holes, in Aid of Shooting Incident Reconstruction

A dissertation submitted for the Degree of Master of Computer Science

W. R. C. Ariyarathna
**University of Colombo School of Computing**
2023

DECLARATION

I hereby declare that the thesis is my original work and it has been written by me in its entirety. I have duly acknowledged all the sources of information which have been used in the thesis. This thesis has also not been submitted for any degree in any university previously.

Student Name: W R C Ariyarathna

Registration Number: 2019/MCS/006

Index Number: 19440065
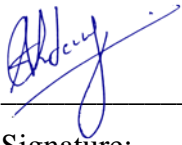
Signature: Date: 28 February 2023

This is to certify that this thesis is based on the work of Mr. W R C Ariyarathna under my supervision. The thesis has been prepared according to the format stipulated and is of an acceptable standard.

Certified by:

Supervisor Name: Dr K D Sandaruwan

Signature: Date: 28 February 2023

ACKNOWLEDGEMENTS

ABSTRACT

Identification of a shooter's location in a shooting incident is a piece of critical information which investigators need to understand for scene reconstruction. Bullet holes and their characteristics play a significant role in tracking bullet paths to their originated locations. Few methods are currently employed to estimate the angle of incidence of fired bullets by means of bullet holes. But each method has its own limitations. The accuracy level of the estimated trajectories depends on many factors. Considering the commonly reported incidents, out of many bullet types and associated target surfaces, the AK family rifles and Zinc coated 1 mm sheet metal are selected for this study.

The study analyzed the special deformation features and metal surface debris spread around the outer perimeter of the bullet impact marks, targeting the determination of incident angle. It also demonstrated two inversely proportional mathematical relationships considering the area of the impact mark and the length of the lead-in crease to the incident angle of the fired AK bullet. And it revealed the possibility of using the bullet impact area to predict the approximated incident angles from 10° to 90° and the usability of lead-in crease length to predict the approximated incident angles below 40°, referring to the AK bullets impact marks identified on Zinc coated 1 mm sheet metal in actual crime scenes.

Keywords:
Shooting incident reconstruction, Forensic evidence, Image processing, Deformation features, Bullet holes, AK rifles, 7.62 x 39 mm ammunition, 1 mm sheet metal

TABLE OF CONTENTS

LIST OF FIGURES

LIST OF TABLES

ABBREVIATIONS

$\pm$	Plus or minus
º	Degree (a unit of measurement of angles)
2D	Two dimensional.
ABFO	American Board of Forensic Odontology
AK-47	Automatic Kalashnikov model in 1947
CDRD	Centre for Defence Research and Development
DSLR	Digital Single-Lens Reflex
EOS	Electro-Optical System
m	Meter
MATLAB	Matrix Laboratory
mm	Millimetre
mm^2	Square millimetre
ms^{-1}	Meter per second
MK II	Mark II (the second version of a product)
RMSE	Root Mean Square Error
USA	United States of America

CHAPTER 1: INTRODUCTION

The process of employing science in the legal system is commonly known as forensic science. A subfield of forensic science is criminalistics. It comprises investigating and recreating shooting incidents and various aspects of criminal investigations (Hueske, 2016). Also, criminalistics is the study of physical evidence that an investigator can see, touch or smell (e.g., hairs, fibres, blood stains, gunpowder residue, footwear impressions, firearms, bullet impact marks and tool marks) ("Forensic science," 2022). The analysis and reconstruction of a shooting incident are much like trying to solve a puzzle using various types of physical evidence found in the scene. When there are missing clues to a puzzle, it can be very frustrating trying to solve it. The same frustration can arise in shooting reconstruction efforts when there are gaps in the associated physical evidence. Therefore, a comprehensive analytical approach starting from the crime scene and continuous efforts towards the off-scene investigation is essential for a successful outcome.

Due to the dynamic nature of the evidence produced, shooting involved crime scenes becomes different to each other. From a particular shooting scene, a crime investigation team will identify, reconstruct and document projectile paths which are called trajectories, referring to the identified impact marks, including bullet penetrating, bullet perforating or ricocheting marks at the points of impact. The careful observation and processing of a scene for relevant physical evidence, including the damages and holes left by projectiles, is essential for reconstructing a shooting incident. Typically, an accurate reconstruction requires locating and gathering relevant forensic evidence at the scene, followed by its investigation in a laboratory ("Forensic Science - Shooting Scene Reconstruction," 2022).

Analyzing defects and holes generated by the bullets fired from weapons can help reconstruct a shooting occurrence. Impact site observations can provide valuable information about the ammunition, the gun, intermediate items in the projectile's path, the direction of the bullet where it originated, the order of firing and many other factors. In some scenarios, it is possible to determine the trajectory of the fired bullet. It can assist in determining the probable location from where a shot was fired. That will lead to other forensically significant evidence, such as empty case traces of the shooter and other suspected weapons.

Figure 1 below illustrates the approximation of a bullet trajectory with a laser. The bullet originated in the doorway (left foreground) and travelled across the apartment to impact the

fireplace (right background). This projectile struck and killed an individual while lying on the sofa bed in front of the fireplace. Multiple impact points showing evidence of contact with the bullet were used to establish this trajectory.
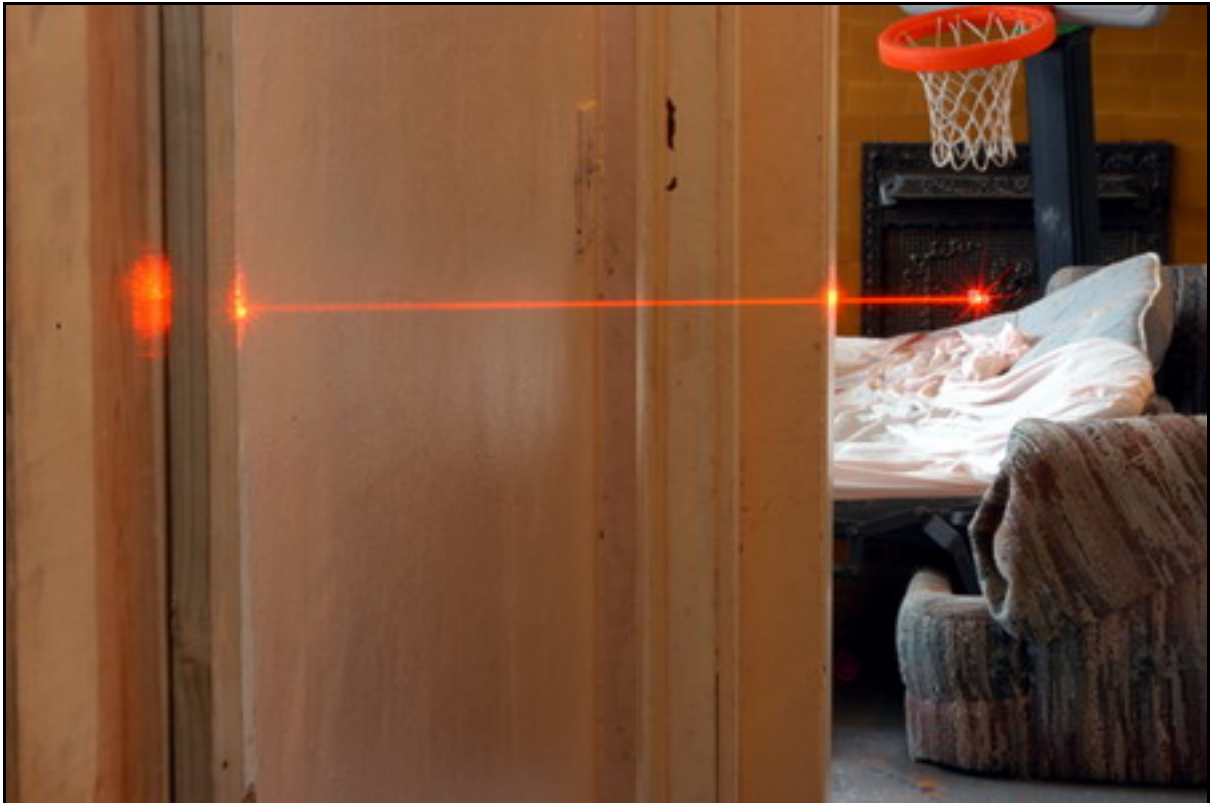
Figure 1.   Approximation of a Bullet Trajectory with a Laser Beam

1.1   Motivation

Compared to the high number of shooting incidents worldwide, it is surprising to find a minimal number of published works on the subject related to incident reconstruction. Although general guidelines on shooting incident reconstruction are available, these cannot always apply to shooting scene investigations as shooting incidents occur under a diverse range of conditions with different bullets, surfaces, weapons etc. In this background, an extensive empirical study has been conducted by the CDRD of the Ministry of Defence. They have introduced an Android application titled "AK Bullet Trajectory Plotter", which uses the full length of AK bullet holes produced or identified on 1 mm sheet metal to assist firearms investigators in understanding and estimating the trajectories of the fired bullets. This project's findings will be utilized to enhance the capability of the existing application to generate more accurately estimated results by investigating a shooting incident through additional aspects with lesser human effort. It will enable them to formulate new capable parameters and guidelines to assist future firearm related crime scene investigations.

1.2   Statement of the Problem

Identifying a shooter's location in a shooting incident is critical information that investigators need to understand to reconstruct a crime scene. Bullet holes and their characteristics play a significant role by assisting to track and recreation of bullet paths. The trajectory rod method, illustrated in Figure 2, is considered the most commonly used method for this.

Figure 2.   Using the Trajectory Rod Method to Understand the Shooter's Location

The trajectory rod method uses two bullet holes, an entry and exit, of a primary and secondary surface of a target to determine the bullet's trajectory. The incident angle is identified based on the directions indicated by the rod inserted through two bullet holes.

When there are two bullet impact holes (entry and exit holes), it is possible to determine the path of a bullet by inserting a rod or a laser beam connecting both holes. However, when there is only one bullet hole to be identified (only an entry hole), the above method cannot be employed. In such a situation determining the bullet's trajectory or angle of incidence becomes a challenging task. The physical properties, such as the shape and the size of the bullet impact mark, are used in such situations. However, certain drawbacks and possible errors have been identified because different bullet-target combinations and ballistics produce various bullet hole characteristics on different surfaces, particular to that bullet-target combination.

In both situations where two bullet holes or a single bullet hole occurred, certain properties of the bullet impact marks are being considered. But there are different visual characteristics and physical parameters in a bullet impact mark that have not yet been assessed for determining the angle of incidence. Considering the above mentioned facts, an image processing method is

proposed to determine the angle of incidence by analyzing the visual characteristics and physical parameters in the presence of a single bullet impact mark.

1.3   Scope

Developed in 1947 and first used by Soviet forces in 1949, the AK-47 assault rifle shown in Figure 3 and its many derivatives are now used in several countries around the world. These guns, popularly known as "AK rifles" or "Kalash rifles", have become an enduring image of contemporary conflicts from major conventional battlegrounds to gangster wars and have been extensively popular among criminals and terrorists. Out of many bullet types and associated target surface types reported in many shooting incidents, the AK family rifles and Zinc coated sheet metal is a commonly encountered firearm and surface combination in shooting incidents worldwide, including in Sri Lanka ("Why did the AK-47 become so popular?," 2016). Therefore the scope of this study is limited to the single bullet holes identified on Zinc coated 1 mm sheet metal surfaces due to the shots fired ten meters (10 m) away from the AK-47 assault rifle with its 7.62 x 39 mm ammunition illustrated in Figure 4.

Figure 3.   An AK-47 Assault Rifle ("Type 56 Assault Rifle," 2022)

Figure 4.   A steel-Cased 7.62 x 39 mm Ammunition ("7.62 x 39 mm," 2022, p. 62)

1.4 Research Aims and Objectives

1.4.1 Aim

This study aims to determine the angle of incidence by digitally quantifying the features of a single bullet hole identified on Zinc coated 1 mm sheet metal surface due to the 7.62 x 39 mm ammunitions fired from AK-47 rifle.

1.4.2 Objectives

The following are the specific objectives of the study:

- Review and analyze the existing methods to determine the angle of incidence and identify the features used when a single bullet impact mark is identified on a 1 mm Zinc coated sheet metal.

- Identify the extra visual characteristics and physical parameters of a single bullet impact mark which have not been considered yet for the determination of the angle of incidence but have the potential to enhance the accuracy of the results.

- Digitally quantify the deformation features identified on a 1 mm sheet metal surface and identify their relationship to the angle of incidence to be referred to as new forensic evidence.

CHAPTER 2: LITERATURE REVIEW

Based on the literature survey, it is observed that early studies were conducted to find alternate methods for more accurate trajectory determinations. As a significant finding of one of such studies, the researchers have observed a correlation, highlighted in Figure 5, between the average full lengths measured manually of the AK bullet holes on 1 mm sheet metal and the angle of incidences.
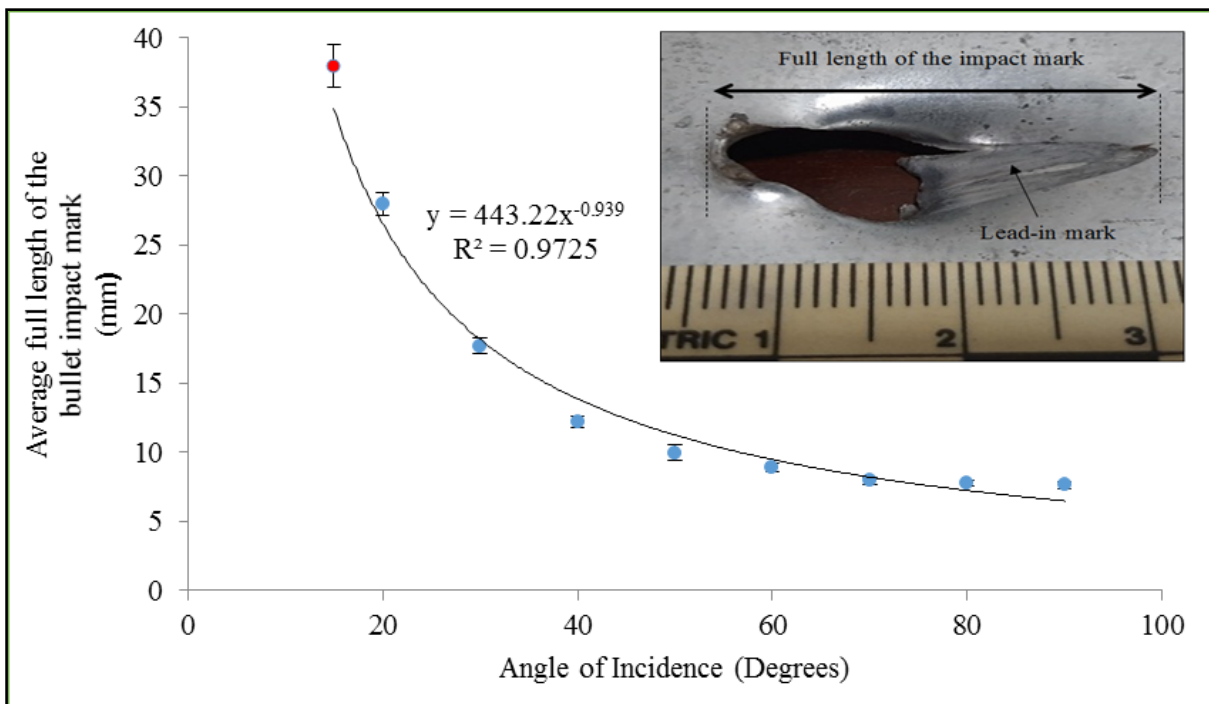
Figure 5.   Identified Relationship between the Full Length of the AK Bullet Impact Mark on 1 mm Sheet Metal and the Angle of Incidences (B. Nishshanka et al., 2021; L. C. B. Nishshanka et al., 2021)

It is observed that in the above study, the researchers have selected only the full length of a bullet impact mark. Also have highlighted a unique impact feature with two heads observed when the incident angle is reduced to 30°, 20° and 15°.

For the low angles of incidents between 3° to 20°, ricochet phenomena were observed (Nishshanka et al., 2020b). A full ricochet was observed there between 3° to 5° degrees, and a partial ricochet / partial penetration phenomenon was observed from 5° to 20°. There, a clear relationship has been demonstrated between the angle of incidence and various measurements relating to the ricochet phenomena, including the lead-in crease length, the length of the first head in the double-headed mark and the entire length of the bullet impact mark. Figure 6 depicts the double-headed impact mark and lead-in crease that appeared on a 1 mm sheet metal.
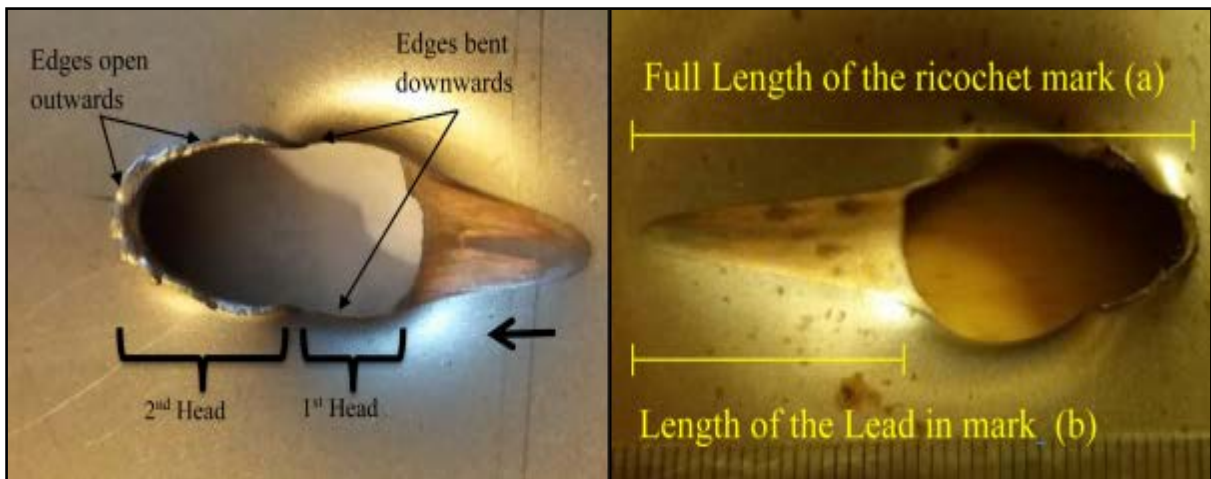
Figure 6.   Representation of Lead-in Crease and Double-Headed Impact Marks Appeared on a 1 mm Sheet Metal (Nishshanka et al., 2020b)

A software solution was designed based (Nishshanka et al., 2020a) on the relationships identified between the lengths of the bullet holes, the lengths of the first head of the double-headed impact marks and the angles of incidence of fired AK bullets. That desktop application proved to be an effective method to quickly provide approximate angles of incidence for AK bullets penetrated through or ricocheting off from 1 mm sheet metal surfaces.

All the above mentioned research studies have used either the lengths measured manually on metal surfaces or the length measured on the captured images from the single bullet impact marks. Capturing those images requires photographs to be taken at 90° perpendicularly to the surface. Errors may be introduced when the length is measured manually or if the pictures are not taken perpendicularly, are of low resolution or too blurry. Also, in higher incidence angles above 60°, the length is sensitive to minor measurement errors, which may result in more considerable differences in accuracy.

Yet another study highlighted that the 2D Ellipse method could be used for understanding the incident angle for crime scene reconstruction when applied to single bullet impact marks located in drywall panels, especially for lower angles of incidence. Figure 7 shows a practical case of using the examples of using Ellipser app to identify the impact angle from a single bullet hole.
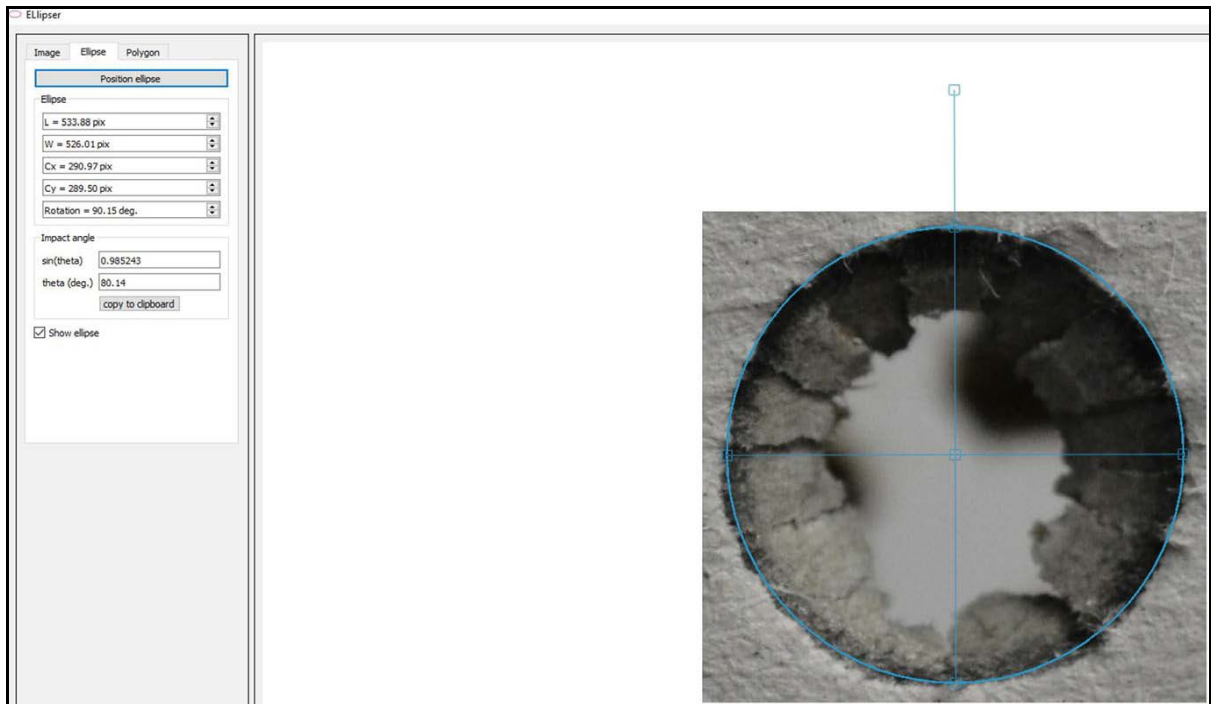
Figure 7.   Calculate the Impact Angle using the Ellipser App Option in CloudCompare Software (Walters and Liscio, 2020)

The major limitation of this method is that the underlined Sine function of the 2D Ellipse method is sensitive to minor measurement errors when the angle of incidence is high (between 70° to 90°), which may result in more considerable differences in accuracy and repeatability calculations. Additionally, applying the 2D Ellipse method requires photographs to be taken at 90° to the surface. Errors may be introduced if the pictures are not taken perpendicularly, low resolution, or too blurry.

Also, it is observed that the fired bullets generate impact marks with different shapes and characteristics on sheet metals when the incidence angle is changed. Figure 8 visualizes the changes in bullet holes and the special deformation features when the incident angle is gradually increasing from 10º up to 90º.

INTENTIONALLY LEFT BLANK.
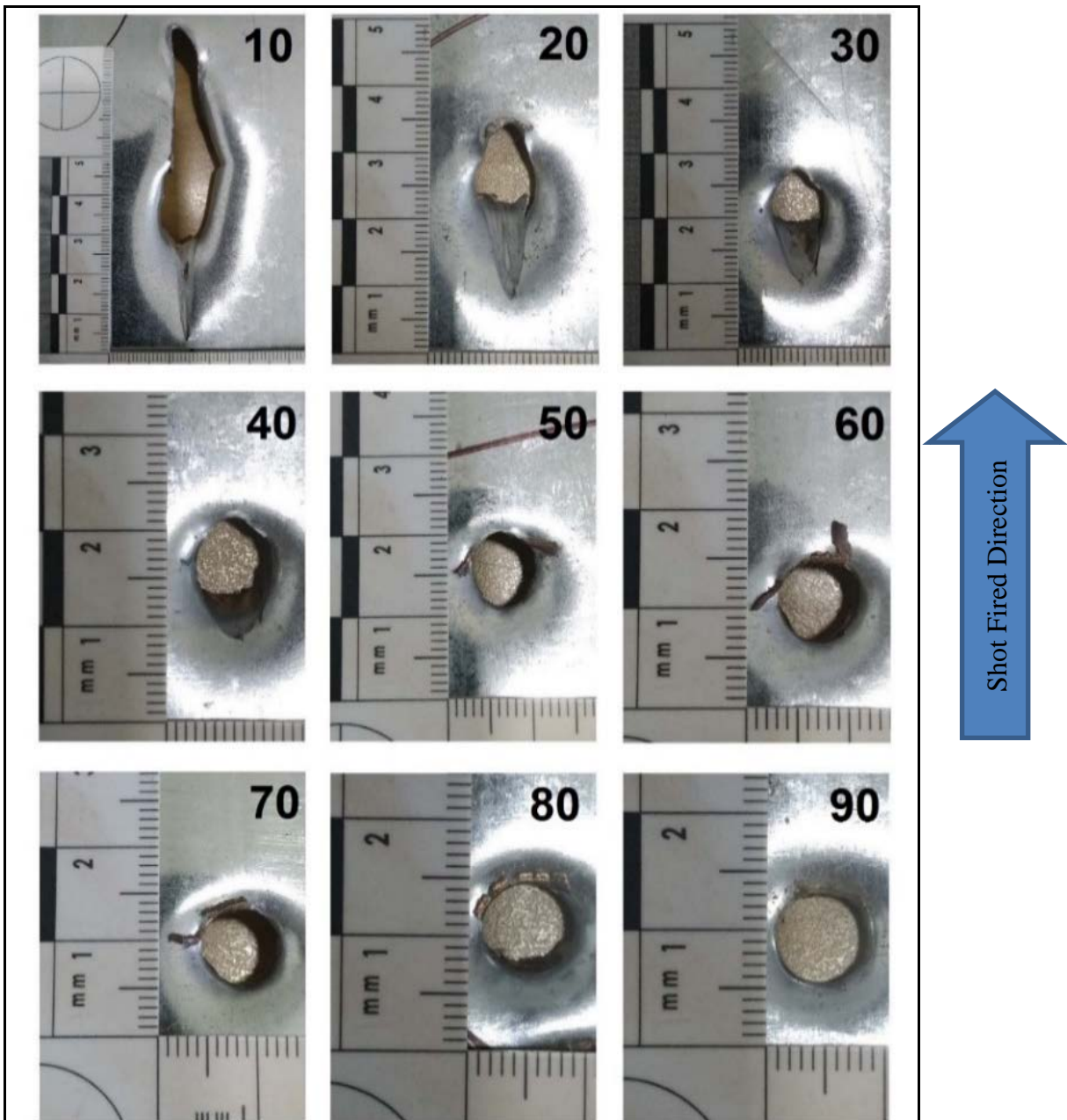
Figure 8.   Changes in Bullet Holes and the Appearance of Special Deformation Features when the Incident Angle Increases from 10º up to 90º (B. Nishshanka et al., 2021)

As highlighted earlier, when there are two bullet impact holes (entry and exit holes), it is possible and easy to determine the path of a bullet by inserting a rod, string or a laser beam connecting both holes. However, when there is only one bullet hole (only an entry hole), the above methods cannot be employed easily and identifying the bullet's trajectory or angle of incidence becomes challenging. To address those challenges, the physical properties of a single bullet impact mark, such as shape and size, are used. However, certain drawbacks and possible errors have been identified due to the reason that different bullet-target combinations and ballistics produce different bullet hole characteristics on different surfaces, particular to that combination.

Few experiments and research studies have been conducted to generate the incident angle when there is a single bullet impact mark to be found on a crime scene. While using the 2D Ellipse method generates accurate results for lower angles. The sine function used in the 2D Ellipse method is sensitive to minor measurement errors when the angle of incidence is high (between 60° to 90°), which may result in more considerable differences in accuracy and repeatability calculations.

An inversely proportional relationship is identified between the angle of incidences from 90° to 15° and the average full-lengths measured from the AK bullet holes on 1mm sheet metal. Here the full length of the bullet impact mark is measured manually on the target surface. That may introduce minor human error to the angle determination process.

Also, capturing the images for the existing incident angle determination methods requires photographs to be taken at 90° to the surface. Errors may be introduced if the pictures are not taken perpendicularly, of low resolution, too blurry or with the noises on the surfaces. All these highlighted drawbacks will introduce minor to large scale inaccuracy results to be referred to by the judicial system.

Even though the distribution of the special deformation features on 1 mm metal surfaces is documented in a few of the previous studies, none of the attempts is made to properly analyze those features targeting the determination of the incident angle. During this study, those visual factors will be analyzed to check the possibility of identifying the incidence angle. Also, it is highlighted that there is a clear relationship between the lead-in crease length and the incident angles below 20°. But even for the naked eye, the lead-in crease is visible from the shots fired up to 40°.

Using the physically available evidence to the maximum level was a primary intention of this study, and all the lead-in crease marks that appeared were tested. Among all the facts, it is identified that none of the attempts was made to analyze the area of a bullet impact mark targeting the incident angle determination. That is not an easy task to do manually. Therefore a digital platform was implemented to address that gap. Successful outcomes of those individual experiments were integrated to introduce a user-friendly software application capable of generating evidence to support the judicial system.

CHAPTER 3: METHODOLOGY

To achieve the aim and objectives of this study it is essential to analyze the single bullet holes identified on Zinc coated 1 mm sheet metal surfaces due to the shots fired from AK-47 assault rifle with its 7.62 x 39 mm ammunition. This project's required firing data samples were available at the Armament and Ballistics Wing of CDRD under the Ministry of Defence, Sri Lanka. Under the supervision of Lieutenant Colonel (Dr) NABMS Nishshanka RSP USP psc SLAC, who is the Chief Coordinator of the Armament and Ballistics Wing of CDRD and the co-supervisor for this project, an additional firing session was conducted at the Sri Lanka Army firing range, Panaluwa to acquire few data samples to verify the results of this study.

3.1   Data Collection

An AK family assault rifle (Type 56-MK II) was fired at 1 mm thick Zinc coated automotive steel metal sheets, held over a range of angles (10° to 90°), and placed at a range of 10 m. A specially designed target tray held the sheet metal at the required angles, and the rifle was fixed to a stable and levelled firing platform to allow the gun to be fired each time horizontally. The level of the barrel was set exactly horizontally to the ground using a masonry level ("STABILA Type 196-2 K Mason Levels," 2022) and was checked regularly between firings. The height of the barrel (from the muzzle end to floor level) was 1.4 m, and the impact point of the target surface was set to align with the barrel height. The horizontal bars of the target frame and firing platform were parallel to the ground, and the level was regularly checked between shots.

1 mm Zinc coated Sheet metal samples of 45 cm x 45 cm were placed in the target tray (sheet metal samples were firmly fitted to the frame of the target tray using four bolts). The angles of the target tray could be adjusted from 0° to 90°. Once the angles were set, the target tray could be locked to ensure no changes to the set angle during firing. An inclinometer ("Divinext Digital Inclinometer Electronic Protractor," 2022) was placed on the sheet metal's surface and set the target tray's angles. The inclinometer precision was ± 0.15°. Ten shots were fired at each angle, starting at 90° and decreasing in 10° regular intervals down to 20°. Due to the large and irregular impact marks generated by the shots fired from 10º angle of incidence, there were only 5 data samples acquired on a 45 cm x 45 cm, 1 mm Zinc coated sheet metal. Due to this, only between 20º and 10º additional ten shots were fired using 15º angle of incidence. Before each shot, the horizontal and vertical levels of the target holders and the

angle of the sheet metal samples were checked and confirmed using an inclinometer. Fired bullets were 7.62 x 39 mm standard Chinese Ball ammunition with mild steel cores/copper jacket and a steel case. The velocities of all fired bullets were measured using a Labradar ("Labradar," 2017) which is a world's latest technology for obtaining high speeds. The average velocity of the fired bullet is observed as 735 ms^{-1}. The experimental arrangement and experimental apparatus are shown in Figure 9.
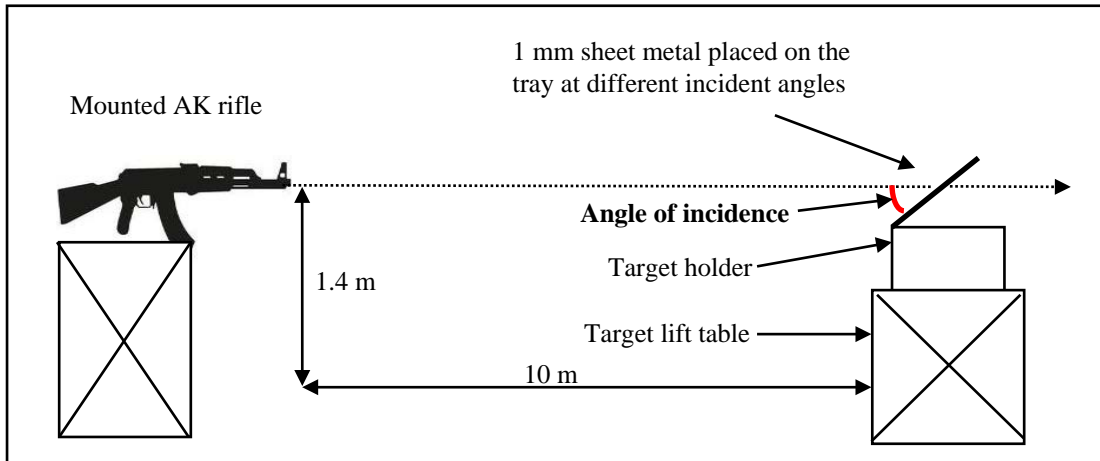
Figure 9.   Experimental Arrangement Used to Collect Firing Data Samples

All the acquired firing data samples from 10º to 90º were photographed and converted into digital form by placing a Forensic ruler ("Forensic Rulers and Scales," 2021) close to the bullet impact mark and using a Canon EOS 90D Camera ("DSLR | EOS 90D | Canon USA," 2020) and stored separately. Figure 10 illustrates a digitized firing data sample from 30º incident angle.

Figure 10.   A Digitized Firing Data Sample from 30º Incident Angle by Placing a Forensic Ruler Close to the Bullet Impact Mark

3.2   Software Implementation

3.2.1 Special Deformation Features Based Implementation

After carefully inspecting the form factors of each bullet impact mark generated from 10° to 90°, it is identified that there are five types of special deformation features and metal surface debris spread around the outer perimeter of the bullet impact marks. Those special deformation features can be named as lead-in crease, double-headed impact marks, raised collars, exit edges bent downward and edges open outward.

Deformation Feature 1: Presence of Lead-in Crease

On the firing data samples collected from 10°, 15°, 20°, 30° and 40°, it is observed that there is a presence of clearly visible lead-in crease from the initial contact point of the bullet with 1 mm Zinc coated sheet metal as illustrated in Figure 11.
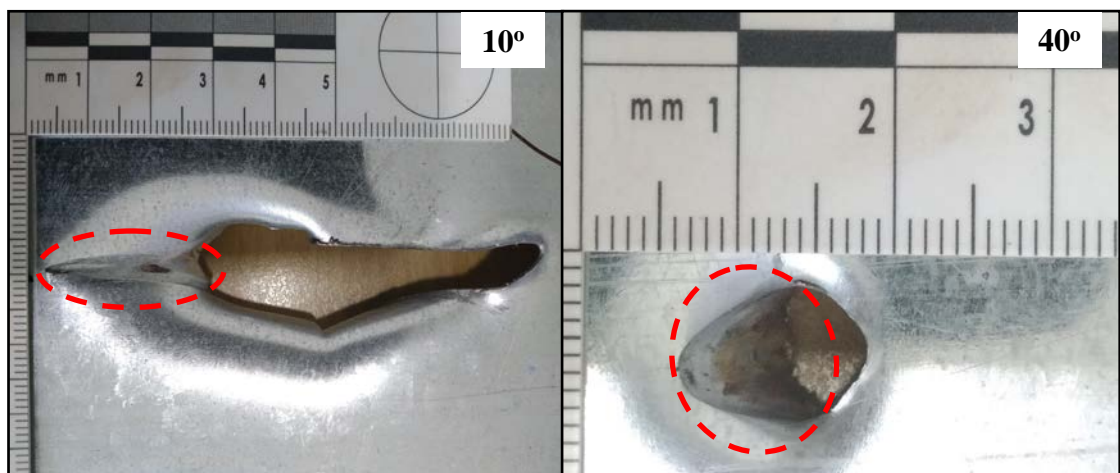
Figure 11.   Lead-in Crease on 1 mm Sheet Metal for 10° and 40° Incident Angles

Deformation Feature 2: Presence of a Double-Headed Impact Mark

On the firing data samples collected from 15°, 20° and 30°, it is observed that there is the presence of a clearly visible double-headed impact mark, as illustrated in Figure 12. Based on the firing data, Nishshanka et al. also highlighted this as a unique feature observed up to a 30° incident angle when AK bullets perforated 1 mm Zinc coated sheet metal (Nishshanka et al., 2020a).
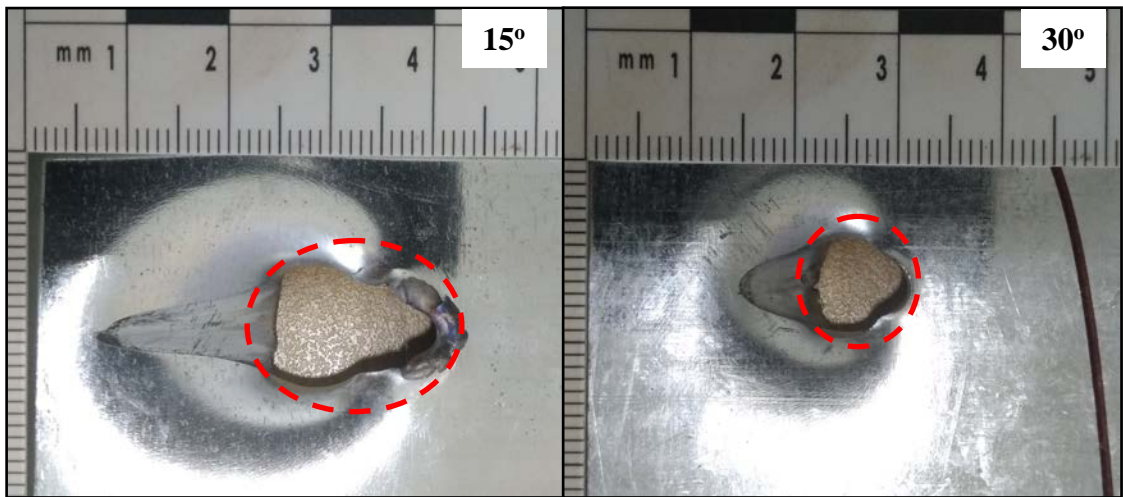
Figure 12.   Double-Headed Impact Mark Appeared on 1 mm Sheet Metal for 15°
and 30° Incident Angles

Deformation Feature 3: Presence of Raised Collars

On the firing data samples collected from 40°, 50°, 60° and 70°, it is observed that there is a presence of clearly visible raised collars at the far end of the initial contact point of the bullet with 1 mm sheet metal, as shown in Figure 13. Nishshanka et al. also highlighted that feature as a special deformation feature observed in the contact of AK bullets and 1 mm Zinc coated sheet metal (Nishshanka et al., 2020a).
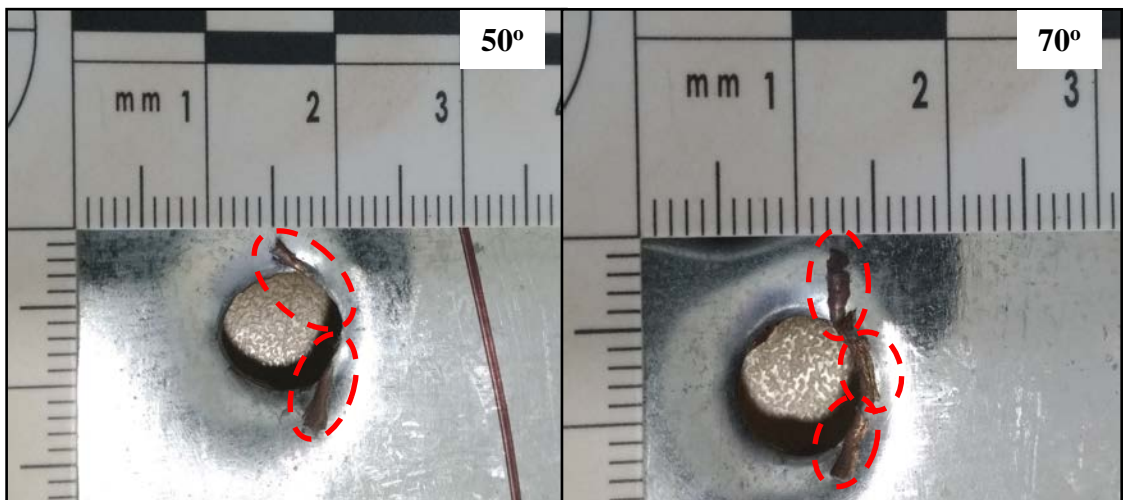
Figure 13.   Raised Collars on 1 mm Sheet Metal for 50° and 70° Incident Angles

Deformation Feature 4: Presence of the Exit Edges Bent Downward

On the firing data samples collected from 30º, 40º and 50º, it is observed that there is the presence of a clearly visible exit edge bent downwards at the far end of the initial contact point of the bullet with 1 mm sheet metal, as shown in Figure 14.
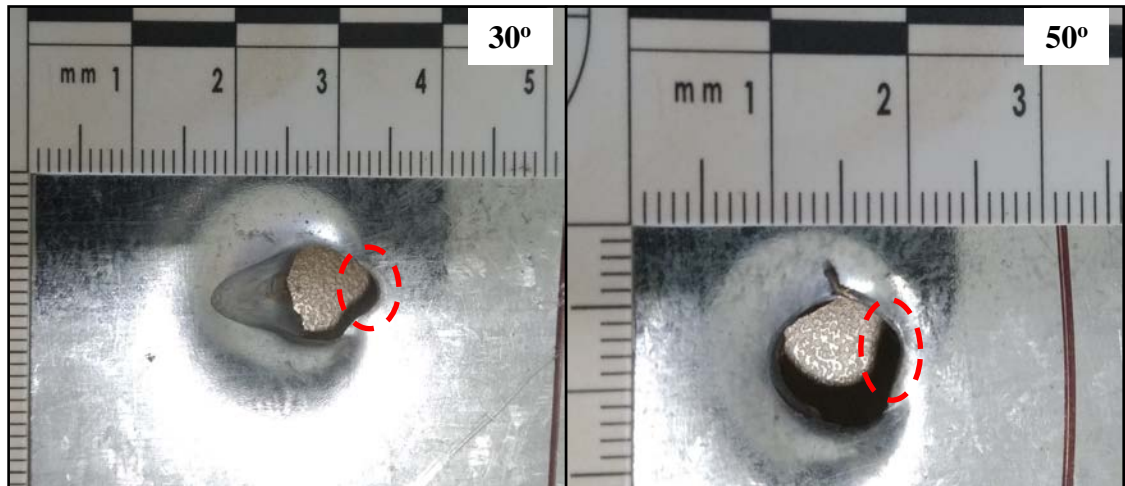
Figure 14.   Exit Edge Bent Downwards, Appeared on 1 mm Sheet Metal for 30º and 50º Incident Angles

Deformation Feature 5: Presence of the Edges Open Outward

On the firing data samples collected from 60º, 70º, 80º and 90º, it is observed that there is a presence of clearly visible edges open outward along the outline of the contact point of the bullet with 1 mm sheet metal as highlighted in Figure 15.
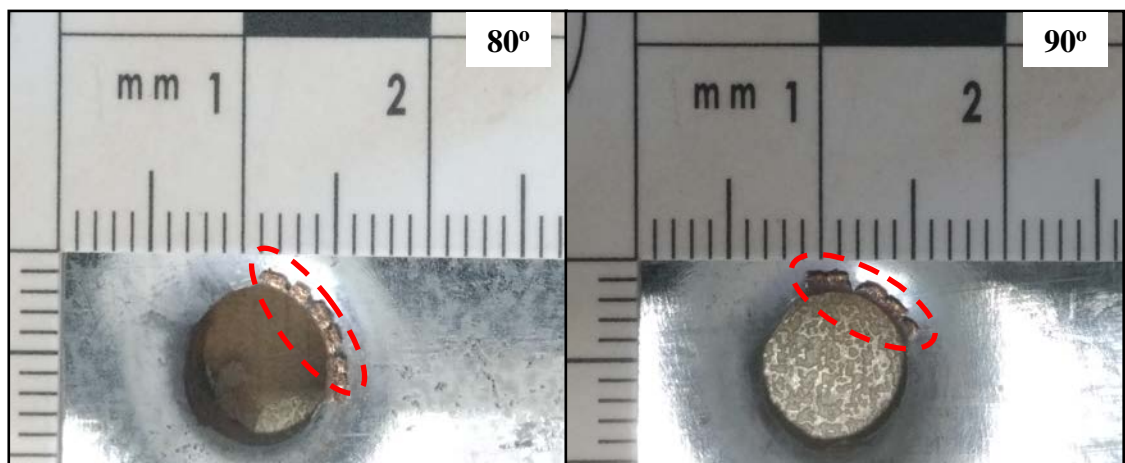
Figure 15.   Edges Open Outward along the Outline, Appeared on 1 mm Sheet Metal for 80º and 90º Incident Angles

Considering the availability of single or multiple deformation features highlighted above, it is possible to get an idea about the possible incident angle before proceeding with the most anticipated digital image processing steps. According to Table 1, it can identify a few combinations of the availability of those five deformation features.

It is also important to note that a ± 5º cone is aligned coaxially along the estimated trajectory during the bullet trajectory estimations process to account for the errors brought on by yaw, precession and nutation of bullets (Haag and Haag, 2011). As illustrated in Figure 16, the software application is developed to "Estimate Incident Angle" after considering the availability of all observed five types of deformation features. Since one deformation feature can appear over a range of incident angles and there could be ± 5º deviation if a bullet may not spin ideally, the software estimating incident angle is also displayed as a range.
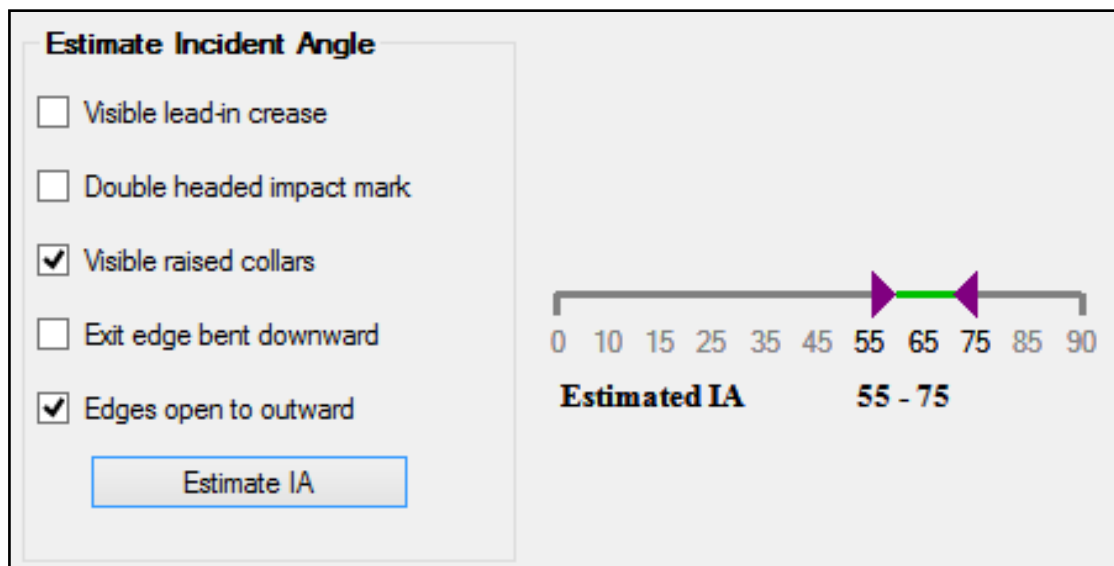
Figure 16.   Implemented Software Option to Estimate Incident Angle in the Presence of Five Types of Special Deformation Features on the Metal Surface

All the firing data samples from 10º to 90º were observed manually, and estimated the angle of incident, according to the identified special deformation features and metal surface debris spread around the outer perimeter of the bullet impact marks. The software generated the result as a range, and those results were saved separately for further evaluation.

3.2.2 Bullet Impact Area Based Implementation

Based on the literature survey, it is identified that the area of a bullet impact mark has not been considered as a potential physical parameter of a single bullet impact mark to determine the angle of incidence. To the naked eye, the area of a bullet's impact mark is inversely proportional to the angle of incidence. Prior to the area calculation, the boundary or the outermost contour of the impact mark is extracted from an image by implementing the GrabCut algorithm ("GrabCut," 2021). GrabCut is an interactive foreground extraction algorithm which was created in 2004 by Carsten Rother, Vladimir Kolmogorov and Andrew Blake ("GrabCut for Automatic Image Segmentation [OpenCV Tutorial]," 2022). The process of extracting the outermost contour of a bullet impact mark and calculating the area of the impact are highlighted in the following flow diagram under Figure 17.
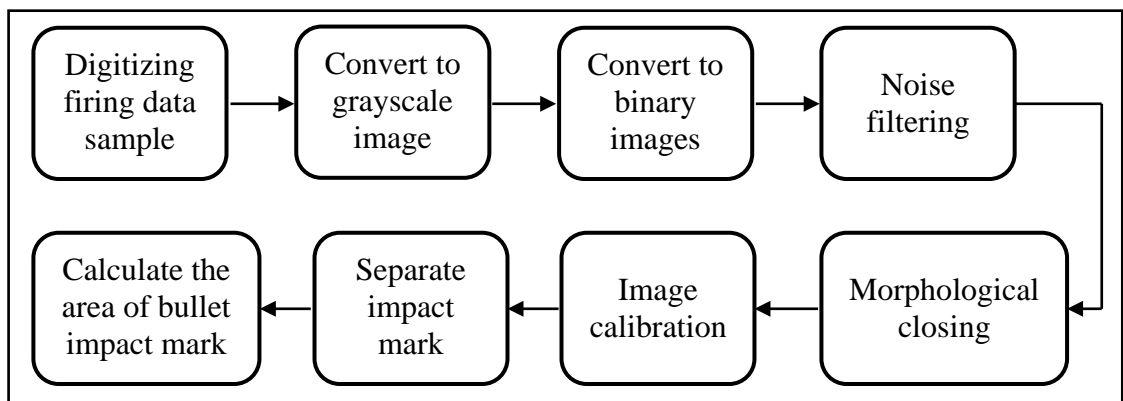
Figure 17.   The Process of Calculating the Bullet Impact Area from Firing Data Samples

Reported consistent relationships between the lengths of the ricochet, perforation marks, lengths of the double-headed impact mark and the bullet's angle of incidence during the two empirical studies (Nishshanka et al., 2020b) and (B. Nishshanka et al., 2021) were the underlying concept for the designing of the initial software application. The software application is developed using Microsoft Visual Studio Community Edition 2013 and the inbuilt Visual C# 2013 package ("Visual Studio," 2022) based on the Microsoft .NET Framework 4.5 (."NET Framework 4.5," 2022). And by linking the Emgu CV ("Emgu CV: OpenCV in .NET (C#, VB, C++ and more)," 2022), which is an open source cross-platform .Net wrapper to the OpenCV ("OpenCV," 2022) image processing library. It allows OpenCV functions to be called from .NET compatible languages.

After digitizing the actual firing data samples by placing a forensic ruler close to the bullet impact mark and using a Canon EOS 90D camera, each image is processed under seven major steps, as indicated above. Each of those seven steps is described here onwards.

Step 1: Convert Colour Images to Grayscale Images

To reduce the colour complexity and for easier visualization, digitized images are initially converted into grayscale images ("The 6 Reasons You Should Convert RGB to Grayscale in Image Editing – C4RE.GR," 2022). For that, digitized images are loaded to the image processing component using "Image<Gray, Byte>" ("Image(TColor, TDepth).Sub Method (Image(TColor, TDepth), Image(Gray, Byte))," 2020) which converts the input images to grayscale images and a generated output is as shown in Figure 18.
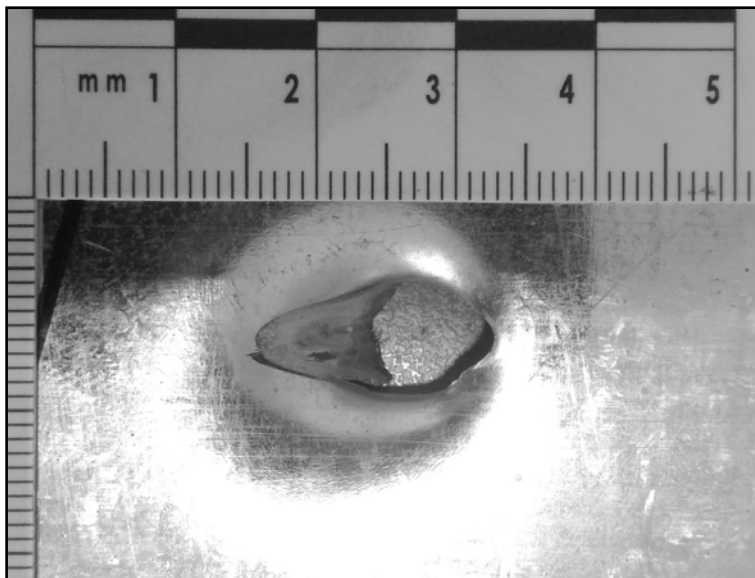
Figure 18.   Generated Grayscale Image from a Bullet Impact Mark of 30° Incident Angle

Step 2: Convert Grayscale Images to Binary Images

Generated greyscale images are then converted into binary images, as shown in Figure 19, using "ThresholdBinary" method of the Emgu CV library ("Image(TColor, TDepth).ThresholdBinary Method," 2020) using a threshold value. An additional option is implemented to change the binary threshold value to generate the most

appropriate binary image that highlights the outermost boundary of the bullet impact mark to a maximum level.
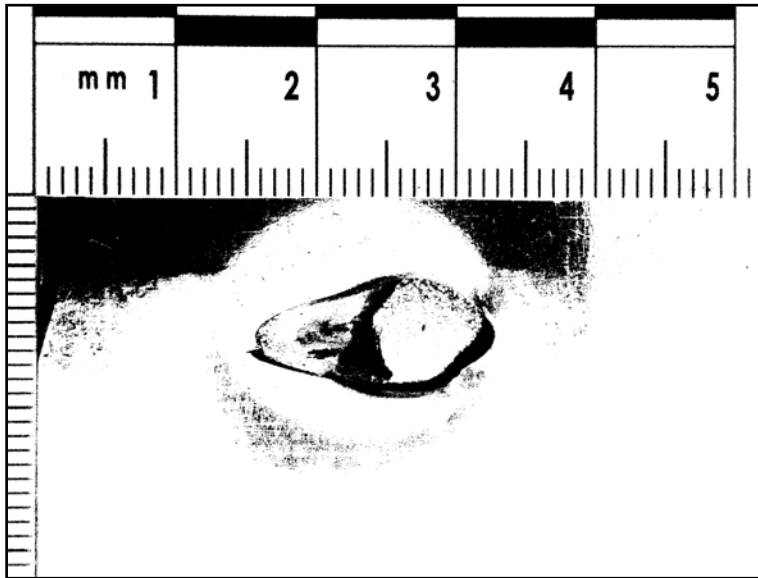
Figure 19.   A Generated Binary Image from a Bullet Impact Mark of 30º Incident Angle

Step 3: Remove Noise from Generated Binary Images

Generated binary images are comprised of unwanted noise data around the bullet impact mark. Considering the nature of that noise, it is identified as the Salt and Pepper noise, which is a certain amount of black dots superimposed on white background ("Salt-and-pepper noise," 2022).

The median filter is one of the well-known filters with good performance in removing Salt and Pepper noise (Gonzalez and Woods, 2008). The median filter substitutes the median value of the relevant window for the centre pixel of size x size neighbourhood. Since the noise black pixels significantly differ from the median pixel value of the filter, it helps to get rid of these noise issues easily.

Considering that for the noise reduction, it is used "SmoothMedian" method of Emgu CV library ("Image(TColor, TDepth).SmoothMedian Method," 2015) with a 3 x 3 Median filter implementation. Smoothen image with reduced salt and pepper noise is highlighted in Figure 20.
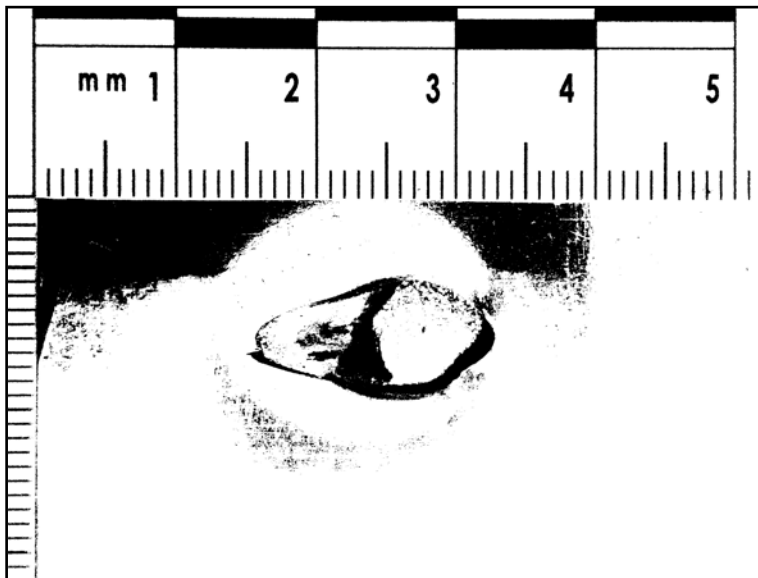
Figure 20.   Noise Filtered Binary Image from a Bullet Impact Mark of 30° Incident Angle

Step 4: Apply Morphological Closing Operation

At the end of the Median filtering process, the outer boundary of the impact marks is more highlighted than in the early stage. But still, there are some gaps between the black pixels along the outer perimeter of the bullet impact mark. The morphological closing operation is implemented there to fill those small gaps in the noise filtered image while preserving the shape and size of the object with the highest concern in the image ("Types of Morphological Operations - MATLAB & Simulink," 2022).

Performing morphological closing operation is defined as a morphological dilation followed by a morphological erosion using the same structuring element for both operations ("Morphology - Closing," 2003). For the dilation operation, it is used "Dilate" method ("Image(TColor, TDepth).Dilate Method," 2015).

For the erosion operation, it is used "Erode" method ("Image(TColor, TDepth).Erode Method," 2015) of the Emgu CV library. For both operations 3 x 3 rectangular structuring element is applied for one time. Changes in the outermost boundary of the bullet impact mark while performing morphological closing are highlighted in Figure 21 and Figure 22.

Figure 21.   A Dilated Binary Image from a Bullet Impact Mark of 30° Incident Angle

Figure 22.   An Eroded Binary after Performing a Dilation (Morphological Closing) Operation

Six standard options, including zoom-in, zoom-out, pan-left, pan-right, pan-up and pan-down, are implemented in the software using inbuilt Windows Forms Designer options that come with Microsoft .NET Framework 4.5 (."NET Framework 4.5," 2022) in order to facilitate the easy visualization of the details of processing images.

Step 5: Calibrate Images to Measure Distance or to Calculate Area

Prior to the area calculation, it is essential to identify the relationship between the image pixel elements and the real world distances. For this software application, that process is defined as "Image Calibration". Real word distances are included in the images at the initial digitization of the firing data samples. All the photos were captured by placing a standard photomicrographic scale, as highlighted in Figure 23, commonly referred to as a forensic ruler ("ABFO No. 2 Photomacrographic Scale," 2022) close to the bullet impact mark and using a Canon EOS 90D Camera.
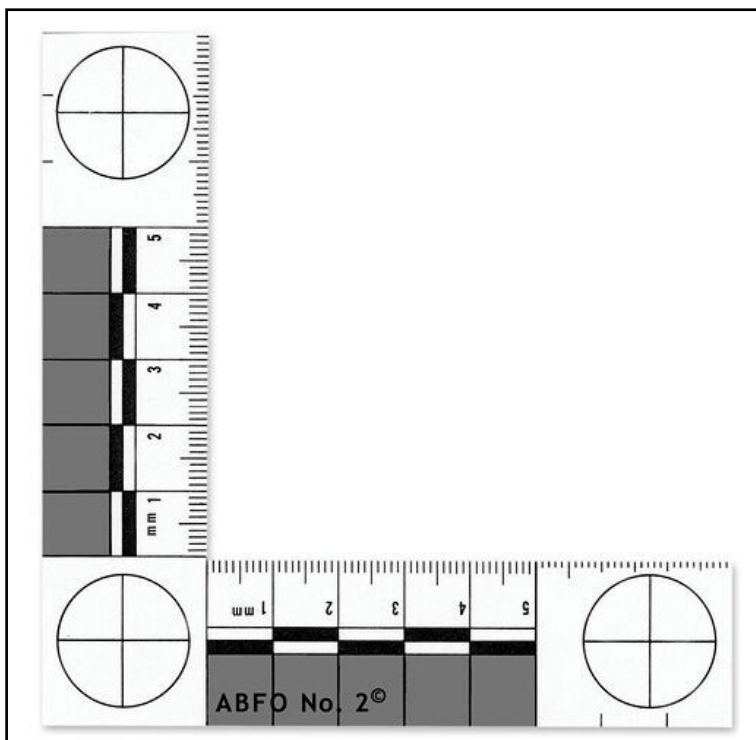
Figure 23.   Photomicrographic Scale ("ABFO No. 2 Photomacrographic Scale," 2022)

Then, the pre-processed binary images are calibrated for further analysis and can be used to measure known distances from the pictures. To begin with the image calibration, a distance is identified which is visible on the image and inserted that distance value to the software in millimetres. Then the same distance is marked on the image along the forensic ruler, and that length appeared on the image as a Yellow colour straight line. The software is implemented to guide through the process with simple instructional messages. Figure 24 illustrates a representation of the final calibration data from the developed software.
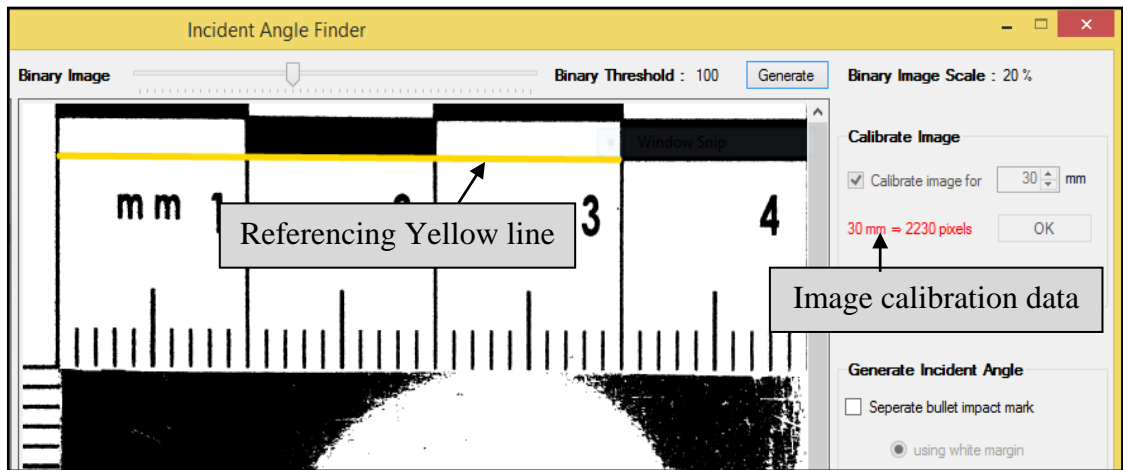
Figure 24.   Representation of Image Calibration Data on the Developed Software

By extracting the edge points' pixel coordinates of the Yellow line followed by a mathematical calculation according to the Pythagoras theorem ("Pythagoras Theorem (Pythagorean) - Formula, Proof, Examples," 2021) the software calculates the pixel distance of the Yellow referencing line. Since that is a known distance marked on the image, the software indicates the final calibration data at the top right area of the application window, as shown in Figure 24. Identified relationship between the image pixel elements and the real world distances is used for all the calculations required for distance measuring on the image and the area calculation of bullet impact marks.

Before the boundary extraction of the bullet impact mark on 1 mm sheet metal, it is required to make sure whether there are any disconnected pixel elements distributed along the possible outermost boundary, as highlighted in Figure 25.
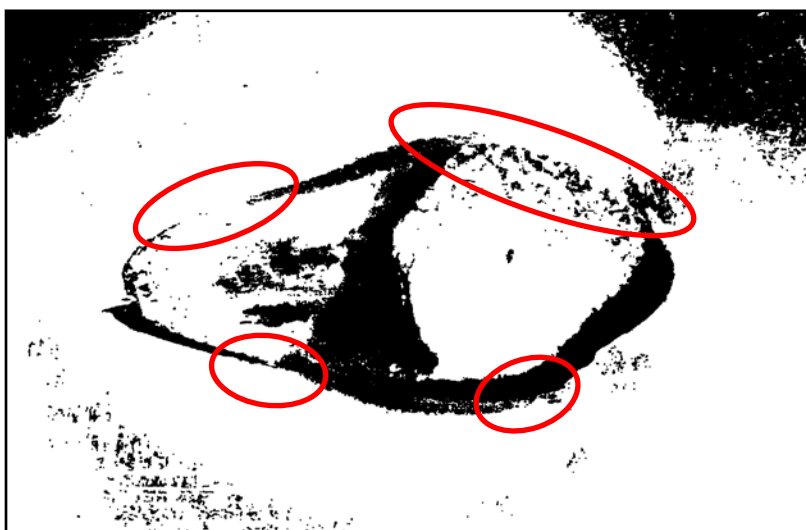
Figure 25.   Distribution of Disconnected Pixels along the Boundary of an Impact Mark

In the presence of such disconnected pixels along the perimeter, incorrect results are generated as the outline of the impact bullet mark, as indicated in Figure 26, since foreground extraction is not happening correctly.
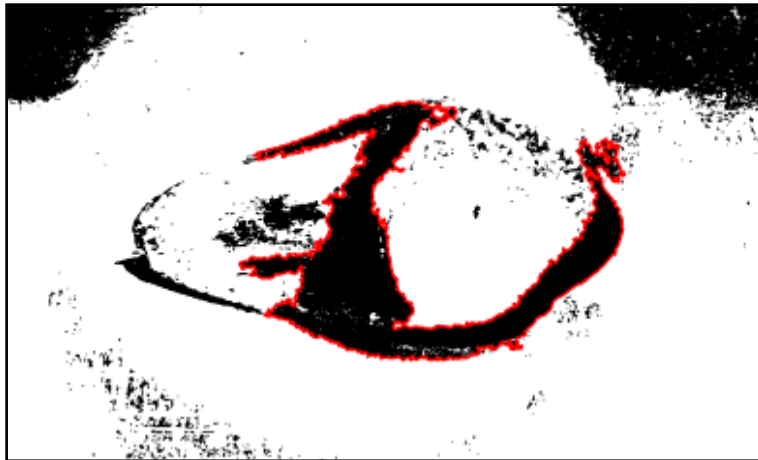
Figure 26.   Incorrectly Identified Outline (in Red Colour) due to the Disconnected Pixels along the Boundary of an Impact Mark

Step 6: Separate Bullet Impact Mark from Background

That issue is addressed by introducing an additional option called "Separate bullet impact mark". It supports drawing smooth arc regions in black and white colours on top of the binary image along the probable outermost boundary of the impact mark. The implementation of that feature is completed by specifying the antialiasing rendering of the lines and curves via the Graphics.SmoothingMode Property of the Microsoft .NET Framework 4.5 ("Graphics.SmoothingMode Property (System.Drawing)," 2022). The output with externally introduced smooth lines and arcs, which highlights the possible outermost boundary, is visualized in Figure 27.
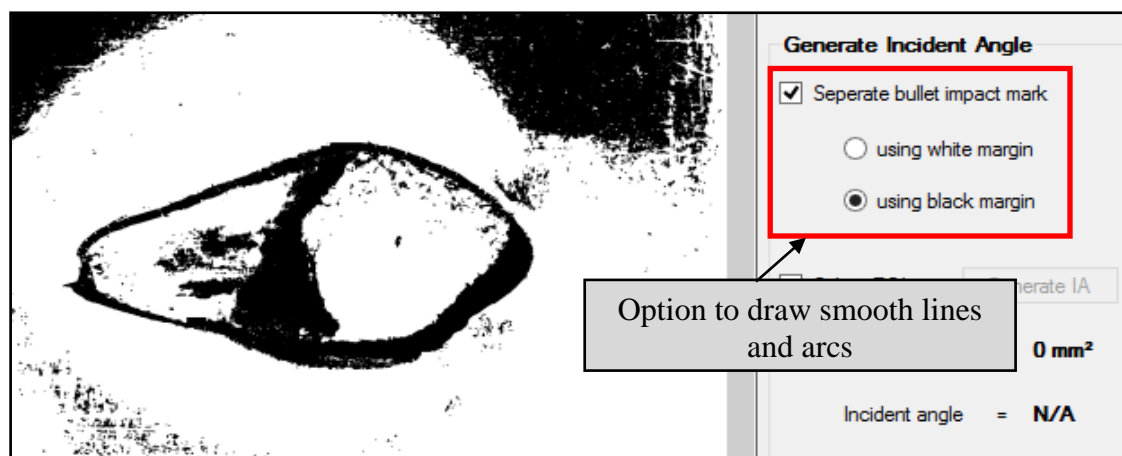
Figure 27.   Possible Outermost Boundary of the Impact Mark with Externally Introduced Black and White Smooth Lines and Arcs

Step 7: Calculate the Area of the Bullet Impact Mark

After all these pre-processing steps, the image is ready to identify the outermost boundary of a bullet impact mark and calculate the area inside. The GrabCut algorithm ("GrabCut," 2021) is used to extract the primary contour of the bullet impact mark. This algorithm generated significantly better results on binary images ("GrabCut for Automatic Image Segmentation [OpenCV Tutorial]," 2022). Implemented version of the GrabCut algorithm follows an interactive process. As shown in Figure 28, the user provides a partial segmentation by drawing a rectangle, enclosing the region of interest where the bullet impact mark is.
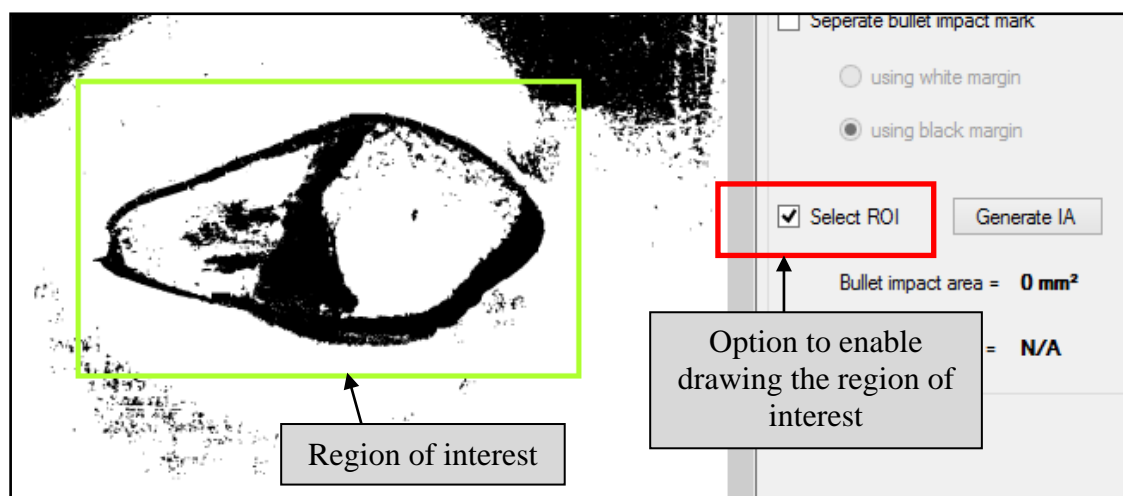
Figure 28.   Initialization of Partial Segmentation by Drawing a Rectangle Enclosing the Region of Interest

After that "GrabCut" method ("Image(TColor, TDepth).GrabCut Method," 2020) of Emgu CV is applied only to the selected region of interest to perform background foreground segmentation. Then CvInvoke.FindContours method ("CvInvoke.FindContours Method," 2019) of the Emgu CV library is applied to the results from early segmentation and retrieves contours from the region of interest of binary image and returns the number of retrieved contours. Out of all the retrieved contours, the biggest contour with the largest area inside is identified using CvInvoke.ContourArea method ("CvInvoke.ContourArea Method," 2020) of Emgu CV library and draw that contour using the "CvInvoke.DrawContours" method ("CvInvoke.DrawContours Method," 2020) of Emgu CV library as highlighted in Figure 29. Then the identified largest contour area is converted to square millimetres (mm^2), an international unit for measuring area, based on the previously calculated image calibration data.

Figure 29.   Identified Largest Contour (in Red Colour) Enclosing the Bullet Impact Mark

All the digitized firing data samples from 10º to 90º were processed using the developed software application according to the seven major steps as indicated above and calculated the area of each bullet impact mark in square millimetres (mm^2) and saved separately for further evaluation.

3.2.3 Lead-in Crease Length Based Implementation

For the low angles of incidents between 3° to 20°, clear relationships have been demonstrated between the angle of incidence and lead-in crease length (Nishshanka et al., 2020b). But based on the visual inspection, it is observed that there is a clearly visible lead-in crease on all the data samples from 10° to 40°. After the calibration of pre-processed binary images, it is possible to measure unknown distances from the pictures. With that motivation, digitized data samples from 10° to 40° are used to measure each lead-in crease that appeared on the data samples.

To measure the lead-in crease length from a calibrated image, there is an option called "Lead-in crease length" under the "Generate Incident Angle" section. After enabling the option, the software provides the necessary instruction to guide through the process of marking the edges of the lead-in crease. As depicted in Figure 30, the marked lead-in crease length along the horizontal axis of the bullet impact mark appears on the image as a Red colour straight line.
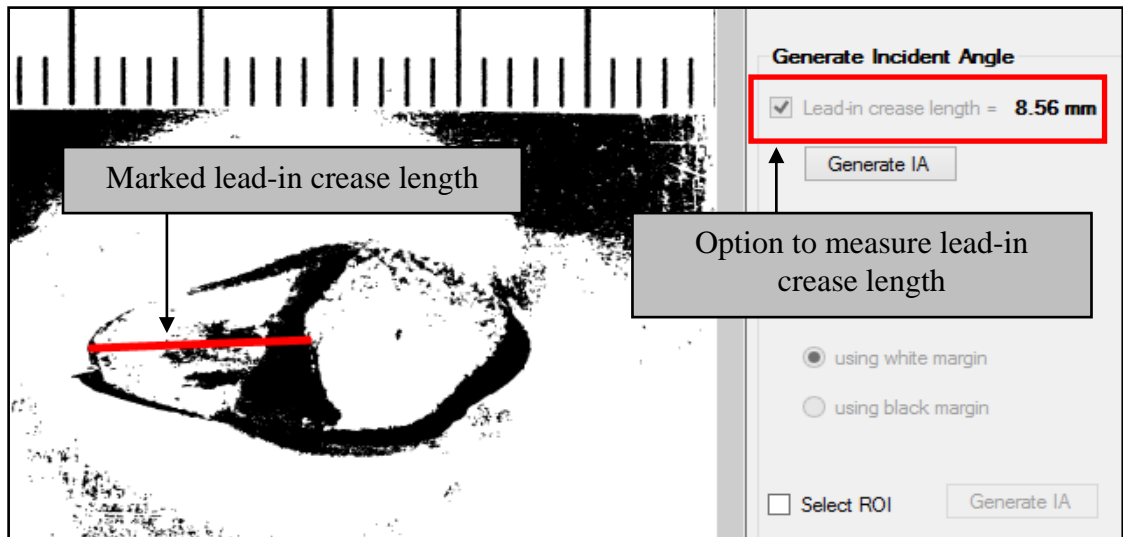
Figure 30. Measuring Lead-in Crease Length along the Horizontal Axis of an Impact Mark

By extracting the edge points' pixel coordinates of the Red line followed by a mathematical calculation according to the Pythagoras theorem ("Pythagoras Theorem (Pythagorean) - Formula, Proof, Examples," 2021), the software calculates the pixel distance of the lead-in crease length highlighted in a Red colour line. Then, referring to the previously identified relationship between the image pixel elements and the real world distances, the software converts the pixel distance of the Red colour line into millimetres (mm) up to two decimal points.

The developed software application processed all the digitized firing data samples from 10º to 40º. Then measured, the lead-in crease length of each bullet impact mark was in millimetres (mm) and saved separately for further evaluation.

CHAPTER 4: RESULTS AND DISCUSSION

4.1 Results of Work

4.1.1 Related to Special Deformation Features

All identified special deformation features and metal surface debris spread around the outer perimeter of the bullet impact marks can be summarized in Table 1, related to the firing data samples from 10º to 90º angle of incidences.

Table 1.   Appearance of Special Deformation Features against the Angle of Incidence from 10º to 90º

Angle of incidence	Visible lead-in crease	Visible double-headed impact mark	Visible raised collars	Visible edges bent downward	Visible edges open outward
10º	Yes	No	No	No	No
15º	Yes	Yes	No	No	Yes
20º	Yes	Yes	No	No	Yes
30º	Yes	Yes	No	Yes	No
40º	Yes	No	Yes	Yes	No
50º	No	No	Yes	Yes	No
60º	No	No	Yes	No	Yes
70º	No	No	Yes	No	Yes
80º	No	No	No	No	Yes
90º	No	No	No	No	Yes

All the identified special deformation features in Table 1 are given a binary value based on their availability (Yes = 1 and No = 0). After converting the generated binary pattern, three common decimal values are generated for the firing data samples from 10º to 90º, as indicated in Table 2. Out of all the associated decimal values, the same results are generated for the data samples from 15º and 20º incident angles. It has happened due to the availability of visible lead-in crease, visible double-headed impact marks, and visible edges open outward in both data samples from 15º and 20º incident angles. Also, it is observed that the exact decimal value is associated with the data samples from 60º and 70º incident angles. It occurred due to the availability of visible raised collars and visible edges open outward in both data samples from 60º and 70º

incident angles. Additionally, it is observed that the same decimal value is generated for the data samples from 80° and 90° incident angles due to the availability of only the visible edges open outward in both data samples.

Table 2.	Binary Representation of the Special Deformation Features and Assigned Range as the Incident Angle

| Actual angle of incidence | Binary representation of the special deformation features | | | | | Associated decimal value | Assigned incident angle range |
	Visible lead-in crease	Visible double-headed impact mark	Visible raised collars	Visible edges bent downward	Visible edges open outward		
10°	1	0	0	0	0	16	0° - 15°
15°	1	1	0	0	1	25	10° - 25°
20°	1	1	0	0	1	25	
30°	1	1	0	1	0	26	25° - 35°
40°	1	0	1	1	0	22	35° - 45°
50°	0	0	1	1	0	6	45° - 55°
60°	0	0	1	0	1	5	55° - 75°
70°	0	0	1	0	1	5	
80°	0	0	0	0	1	1	75° - 90°
90°	0	0	0	0	1	1	

When assigning the incident angle ranges in Table 2, according to the deformation features, a ± 5° range accounts for the errors brought on by yaw, precession and nutation of bullets trajectories (Haag and Haag, 2011). The "7.62 x 39 mm Ammunition's Incident Angle Finder" software application is equipped with these assigned incident angle ranges.

4.1.2 Related to Lead-in Crease Length

All the digitized firing data samples from 10° to 40° were processed using the developed software application, measured the lead-in length of each bullet impact mark in millimetres (mm), and saved separately. A summary of the average lead-in length of each bullet impact mark against the angle of incidence is shown in Table 3.

Table 3.   Average of the Measured Lead-in Crease Length of the Impact Mark and Incident Angle of Bullets from 10º to 40º

The known angle of incidence	Number of processed data samples	Average lead-in crease length (mm)
10º	5	27
15º	10	19
20º	10	15
30º	10	9
40º	10	6

Using the same data set related to average lead-in crease length, an exponential curve fitting is performed in MATLAB R2015a ("MATLAB - MathWorks," 2022), and a graphical illustration of the result is shown in Figure 31. A tightly coupled, inversely proportional mathematical relationship is observed between the angle of incidence and the average lead-in crease length of the bullet impact marks for the firing data samples from 10º to 40º.
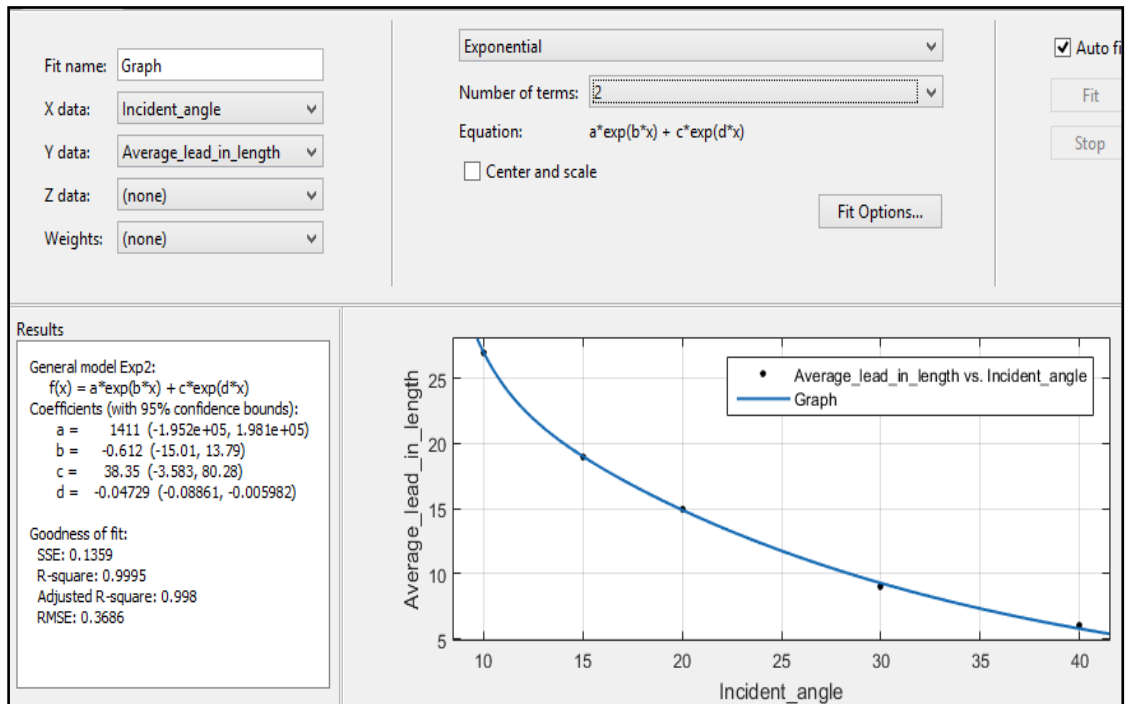
Figure 31.   Mathematical Relationship of Incident Angle to the Average Lead-in Crease Length of Bullet Impact Marks

To apply this mathematical relationship in practical problems, unknown incident angles need to be identified in the presence of a bullet impact mark. Using the same data set and inbuilt features of the curve fitting option of MATLAB R2015a, it is easy

to identify the relationship between the average lead-in crease lengths of bullet impact marks to the incident angle, as illustrated in Figure 32. The "7.62 x 39 mm Ammunition's Incident Angle Finder" software application is equipped with this exponential equation.
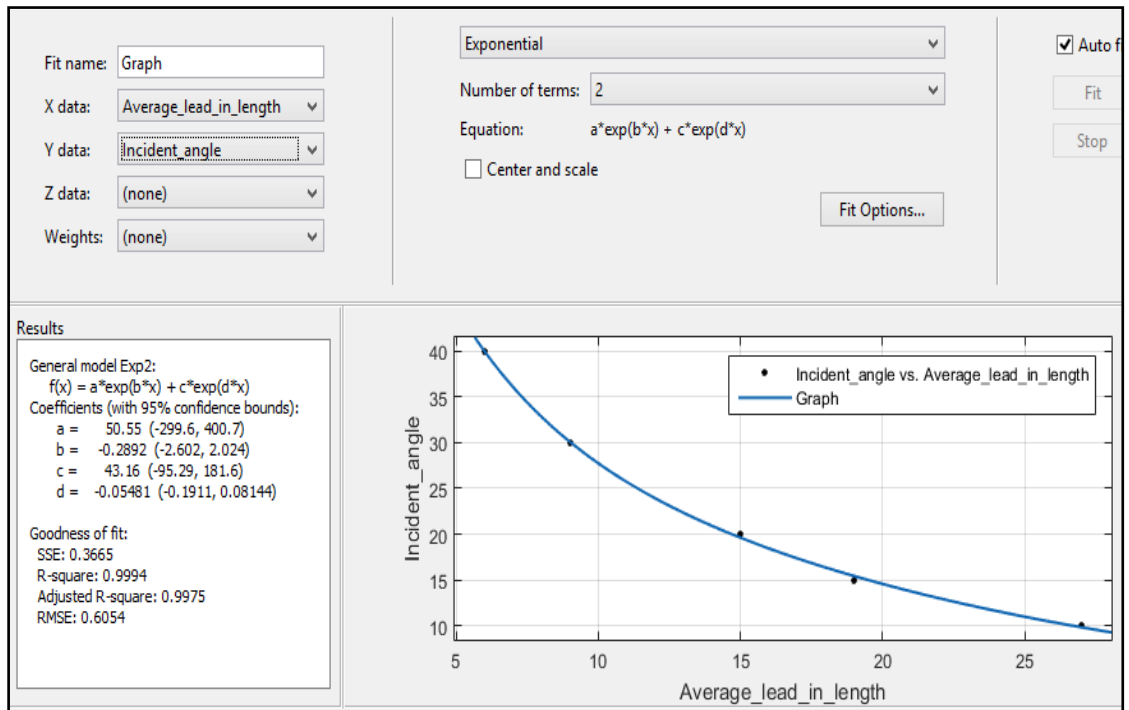
Figure 32.   Mathematical Relationship of Average Lead-in Crease Length of Bullet Impact Marks to the Incident Angle

4.1.3 Related to the Impact Area

All the digitized firing data samples from 10° to 90° were processed using the developed software application according to the seven major steps as indicated above and calculated the area of each bullet impact mark in square millimetres (mm^2) and saved separately. A summary of the average area of each bullet impact mark against the angle of incidence is shown in Table 4. Using the same data set related to the average area of the impact mark, an exponential curve fitting is performed in MATLAB R2015a ("MATLAB - MathWorks," 2022), and a graphical illustration of the result is shown in Figure 33. A tightly coupled, inversely proportional mathematical relationship is observed between the angle of incidence and the average area of the bullet impact marks.

Table 4.   Average of the Calculated Area of the Impact Mark and Incident Angle of Bullets from 10º to 90º

The known angle of incidence	Number of processed data samples	The average area of the impact mark (mm²)
10º	5	669
15º	10	263
20º	10	161
30º	10	99
40º	10	77
50º	10	67
60º	10	58
70º	10	54
80º	10	50
90º	10	49

Figure 33.   Mathematical Relationship of Bullet Incident Angle to the Average Area of the Bullet Impact Marks

To apply this relationship to solve practical problems, unknown incident angles need to be identified in the presence of a bullet impact mark. Using the same data set and inbuilt features of the curve fitting option of MATLAB R2015a, Figure 34 illustrates

the relationship identified between average areas of bullet impact marks to the incident angle. The "7.62 x 39 mm Ammunition's Incident Angle Finder" software application is enhanced based on this exponential equation.
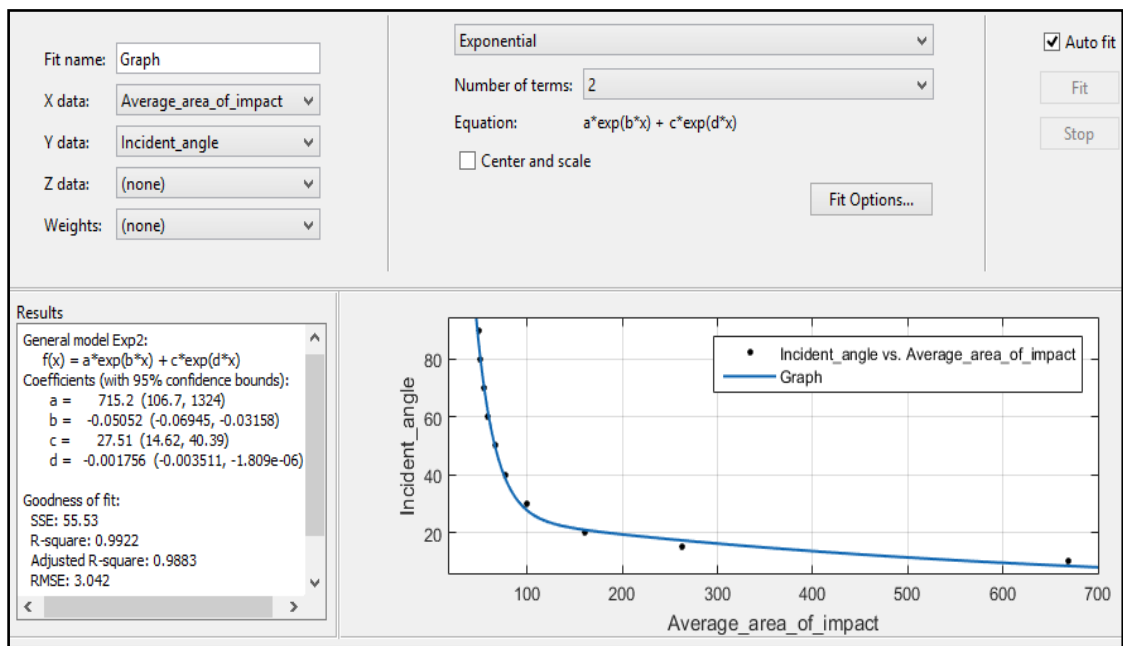
Figure 34.   Mathematical Relationship of the Average Area of the Bullet Impact Marks to the Incident Angle

4.2   Evaluation

A New test procedure is conducted in order to evaluate the practical applicability of identified special deformation features, the mathematical relationship of lead-in crease length to the incident angle and the relationship of the area of the bullet impact marks to the incident angle. The test is conducted using the firing data samples captured using a van door with a 1 mm sheet metal body.

For that firing data collection session, a different AK rifle with the same steel core ammunition were used to fire at the van door, which was placed at 10 m to varying angles from the shooter's position. In that setup, seven 7.62 x 39 mm AK ammunitions were fired for each angle in 10° intervals from 10° to 90°. Pictures taken from that data collection session are shown in Figure 35.

Figure 35.　Captured Firing Data Samples Using a Van Door Made of 1 mm Zinc Coated Sheet Metal

4.2.1 Evaluation of Special Deformation Features Based Implementation

All new test data samples on the van door were used for this evaluation. For each image software application is populated with inputs considering the availability of single or multiple deformation features called lead-in crease, double headed impact mark, raised collars, exit edge bent downward, and edges open outward. All the data samples were correctly categorized to the closest range, related to their incident angles, as shown in Table 5.

Table 5.　The Developed Software Estimated Range as the Angle of Incident

The known angle of incidence	Number of tested data samples	The estimated range for the incident angle
10º	7	0º - 15º
20º	7	10º - 25º
30º	7	25º - 35º
40º	7	35º - 45º
50º	7	45º - 55º
60º	7	55º - 75º
70º	7	55º - 75º
80º	7	75º - 90º
90º	7	75º - 90º

Due to the availability of visible raised collars and visible edges open outward, all data samples from 60º and 70º incident angles were classified correctly into the 55º - 75º range. Also, due to the availability of only the visible edges open outward, all data samples from 80º and 90º incident angles were classified correctly into the 75º - 90º range. Other than the two common cases highlighted above, all the data samples from 10º, 20º, 30º, 40º and 50º were correctly classified into the closest ± 5º range.

Based on the results, it is observed that an in-depth visual analysis of the special deformation features and metal surface debris spread around the outer perimeter of the bullet impact marks can be used as a viable solution. It can produce a significant result with high accuracy to narrow the scope and identify the possible incident angle for a fired 7.62 x 39 mm AK ammunition.

4.2.2 Evaluation of Lead-in Crease Length Based Implementation

The firing data samples from 10º to 40º used for this evaluation due to lead-in crease clearly appeared only on that range. After the digitization of the actual firing data samples from 10º to 40º by placing a forensic ruler close to the bullet impact mark and using a Canon EOS 90D camera, each image is calibrated to measure distances. After the calibration, it is possible to measure the length of the lead-in crease mark along the horizontal axis of the bullet impact mark.

Then the angle of incidence is computed according to the mathematical relationship of the average lead-in crease length of bullet impact marks to the incident angle shown in Figure 32. All generated results based on the lead-in crease length of impact marks are indicated in Table 6.

Table 6.   Average of the Computed Incident Angle Based on the Length of Bullet Lead-in Crease Mark

Incident angle	Number of processed data samples	Average of the computed incident angles
10º	7	9.71º
20º	7	20.00º
30º	7	30.86º
40º	7	40.57º

The average angle of incidence is calculated for all the estimated angles according to the relationship of the average lead-in crease length of bullet impact marks to the incident angle. Then, the difference between the computed average angles and the actual incident angles is calculated. The difference from the mean compared to the actual angles of incidence of fired AK bullets are illustrated in Figure 36.
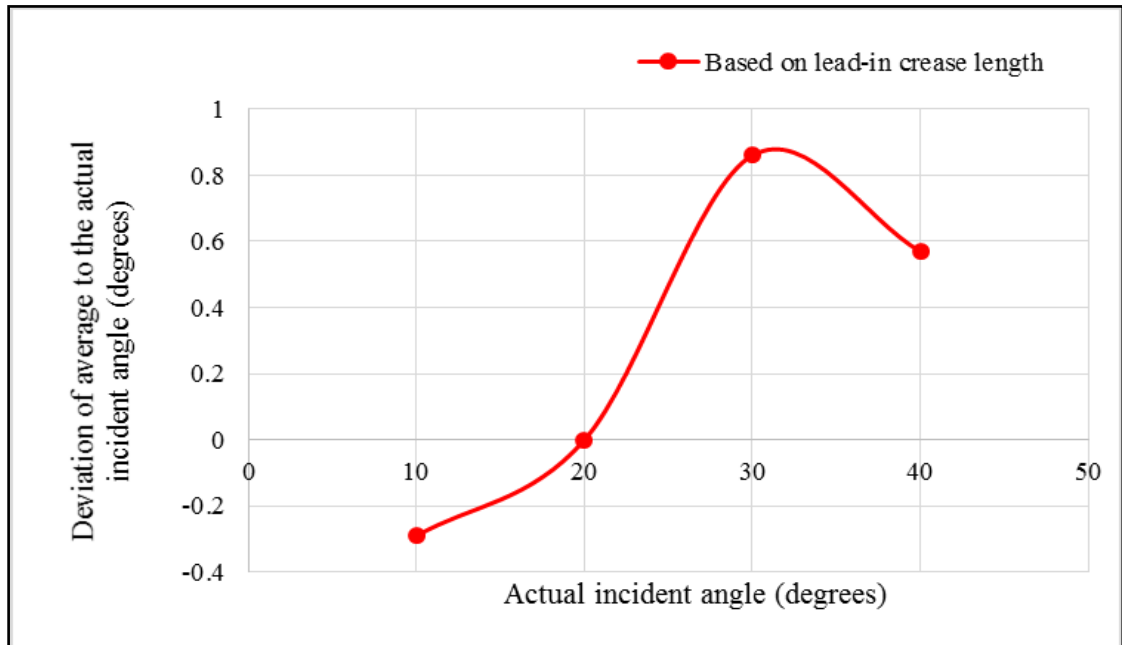
Figure 36.　　Difference to the Mean of the Computed Angle of Incidence, Using the Relationship of Average Lead-in Crease Length to Incident Angle of Fired AK Bullets

It is highlighted that the estimated incident angles, according to the new relationship of average lead-in crease length to the incident angle, are within $\pm 1^{\circ}$ range of the actual incident angles. With that accuracy, this method can be considered a better approach for identifying low incident angles less than or equal to 40°. A previous study proved a similar kind of relationship for determining a low incident angle between 3° and 21° (Nishshanka et al., 2020b). Based on the newly established relationship from this study, the earlier identified range can extend up to 40° to determine the angle of incidence in the presence of a clearly visible lead-in crease mark.

Based on the results, it is observed that a new relationship of average lead-in crease length to the incident angle of fired AK bullets can be used as a viable alternative solution which is capable of producing significant results with higher accuracy ($\pm 1^{\circ}$ error margin) for identifying incident angles below 40° for a fired 7.62 x 39 mm AK ammunition.

4.2.3 Evaluation of Bullet Impact Area Based Implementation

After digitising the actual firing data samples by placing a forensic ruler close to the bullet impact mark and using a Canon EOS 90D camera as highlighted under the "Methodology", each image is processed according to the seven major steps as indicated in Figure 17. In the end, it is possible to extract the outer boundary and calculate the impact area of each shot fired, followed by computing the angle of incidence according to the relationship of the average area of the bullet impact marks to the incident angle shown in Figure 34. All generated results based on the area of impact marks are indicated in Table 7.

Table 7.   Average of the Computed Incident Angle Based on the Area of Bullet Impact Mark

Incident angle	Number of processed data samples	Average of the computed angles
10º	7	8.86º
20º	7	21.14º
30º	7	28.43º
40º	7	39.43º
50º	7	48.86º
60º	7	61.71º
70º	7	69.43º
80º	7	80.86º
90º	7	87.29º

Along with the new relationship of the average area of the bullet impact marks to the incident angle, previously identified full length based relationship (B. Nishshanka et al., 2021; L. C. B. Nishshanka et al., 2021) and commonly used 2D Ellipse method (Walters and Liscio, 2020) were used to estimate the angles of incidences using the same data set acquired on the van door, and the estimated values were recorded. The average angle of incidence is calculated for all the estimated angles under the Ellipse method, full impact length based method, and impact area based approach. Then, the difference between the average angles and the actual incident angles is calculated. The comparison of the difference to the mean reported in the three methods compared to the actual angles of incidence of fired AK bullets is illustrated in Figure 37.
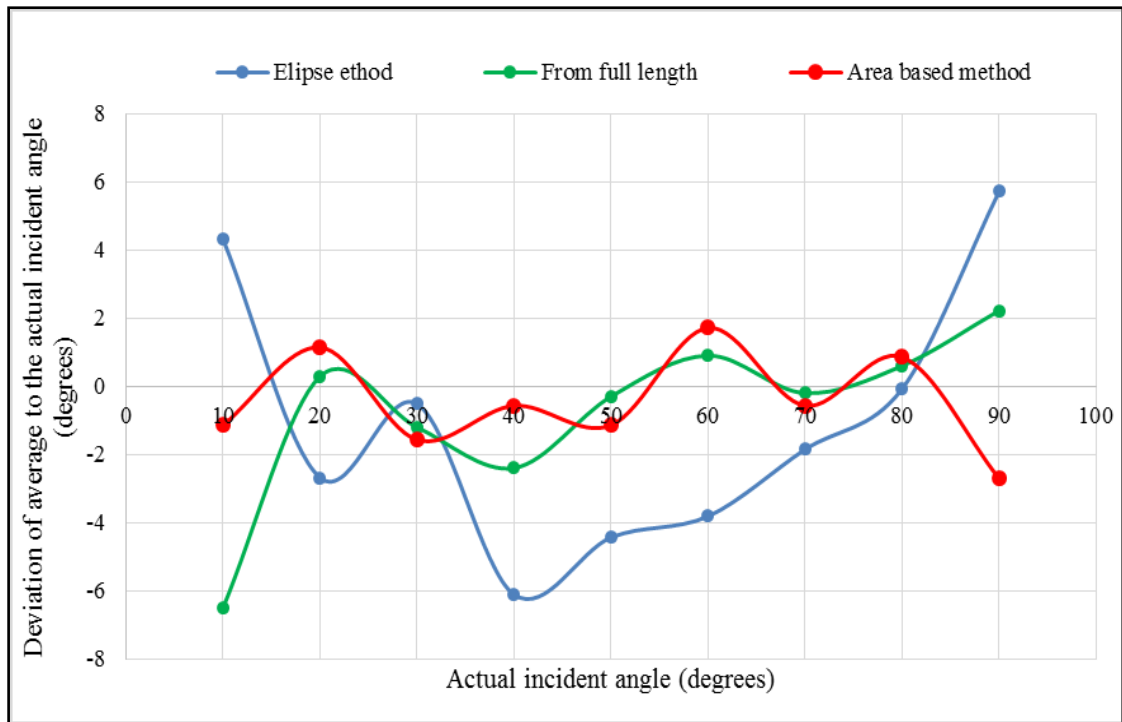
Figure 37. Comparison of Difference to the Mean in the Estimated Angles of Incidence, Using Three Methods Compared to the Actual Angles of Incidence of Fired AK Bullets

Using the same dataset related to Figure 37, Root Mean Square Error (RMSE) is calculated from all the estimated angles under the Ellipse method, full impact length based method, and impact area based approach, as summarised in Table 8. RMSE indicates how concentrated the computed angle data is around the actual incident angles ("RMSE," 2022).

Table 8. Root Mean Square Error Calculated for all the Computed Angles under the Ellipse Method, Full Impact Length Based Method and Impact Area Based Approach

Method	*Root Mean Square Error*
Ellipse method	3.857159º
Full impact length based method	2.489143º
Impact area based approach	1.41505º

For a particular incident angle, different results are estimated as the incident angle due to the slight deviations that occurred to the bullet trajectory on its way to a surface. Various angles of the impact are caused by yaw, precession and nutation of the bullets prior to impact (Haag and Haag, 2011). As well as the uneven curved shape of the van

door might be another reason for estimating different results for the same fired angle. It is also important to note that a ± 5° cone is aligned coaxially along the estimated trajectory during the bullet trajectory estimations process to account for the errors brought on by yaw, precession and nutation of bullets.

Also, it is highlighted that the computed incident angles, by applying the new mathematical relationship of the average area of the bullet impact marks to the incident angle, has the lowest Root Mean Square Error value, which is better when compared to the results generated by the traditional 2D Ellipse method. Also, the new method based results closely align with the results generated according to the previously proven full length based relationship (B. Nishshanka et al., 2021; L. C. B. Nishshanka et al., 2021).

Based on the results, it is observed that the new mathematical relationship of the average area of the bullet impact marks to the incident angle is better than the Ellipse method and full length based method. Therefore it can be used as a viable solution which is capable of producing a significant result with high accuracy to narrow down the scope and to identify the probable incident angle for a fired 7.62 x 39 mm AK ammunition.

4.3   Conclusion

This study was conducted to identify the extra visual characteristics and physical parameters of a single bullet impact mark which have not been considered yet for the determination of the angle of incidence but have the potential to enhance the accuracy of the results in the bullet trajectory reconstruction process. 7.62 x 39 mm AK bullet impact marks captured from 10° to 90° firing angles on 45 x 45 cm Zinc coated 1 mm sheet metal were analysed for this purpose.

After carefully inspecting the form factors of each bullet impact mark generated from 10° to 90°, it is identified that there are special deformation features and metal surface debris spread around the outer perimeter of the bullet impact marks. Those special deformation features are lead-in creases, double headed impact marks, raised collars, exit edges bent downward and edges open outward.

Also, it is identified that the spread of those deformation features over the different incident angles from 10º to 90º. It is determined that an in-depth visual analysis of the special deformation features and metal surface debris spread around the outer perimeter of the bullet impact marks is a better starting point with high accuracy to understand the incident angle before processing the AK bullet impact marks with modern digital techniques.

It is identified that there is a strong inversely proportional mathematical relationship between the angle of incidence from 10º to 40º and the lead-in crease length of the bullet impact marks. Early studies highlighted this kind of relationship from 3º to 21º incident angle. This study proved that 3º to 21º range could be extended and newly identified mathematical relationship is a viable alternative solution with higher accuracy (± 1º error margin) to identify incident angles below 40º in the presence of clearly visible lead-in crease mark from a fired 7.62 x 39 mm AK ammunition to Zinc coated 1 mm sheet metal.

The study revealed a tightly coupled, inversely proportional mathematical relationship between the angle of incidence from 10º to 90º and the area of the bullet impact marks. To this date, that kind of mathematical relationship has not been reported or used in the field of shooting incident reconstruction concerning the 7.62 x 39 mm AK bullets and Zinc coated 1 mm sheet metal involved in the bullet-surface combination. Also, a proper set of image pre-processing steps were identified to extract the outer boundary and calculate the area of a bullet impact mark. Then proved that identified mathematical relationship is a viable alternative solution capable of producing a significant result with high accuracy to narrow down the scope and to understand the probable incident angle for a fired 7.62 x 39 mm AK ammunition on Zinc coated 1 mm sheet metal.

After combining the special deformation feature analysis and two mathematical relationships, "7.62 x 39 mm Ammunition's Incident Angle Finder" desktop software application is developed as an image processing tool to determine the angle of incidence for 7.62 x 39 mm AK ammunition caused bullet holes on Zinc coated 1 mm sheet metal, in aid of shooting incident reconstruction.

4.4 Future Work

Crime scene investigation is a critical process interconnected with the legal system. Therefore the accuracy of the generated results plays a significant role. By now, there is a possibility of generating results within $\pm 5^{\circ}$ range from the actual incident angles. Even that $\pm 5^{\circ}$ range might lead to substantial errors when dealing with crime scenes in dense or urban areas. Using microscopic level images, the software can calibrate the image accurately. Accurate calibration data is always capable of generating more accurate results.

Also, through the microscopic level analysis, an investigator might be able to identify various additional deformation features, and metal surface debris spread around the bullet impact marks. Incorporating those analytical data would benefit more in the incident angle determination process. For this study, it is used data samples from 10° intervals up to 90°. If firing data can be collected for each angle below 90°, the identified mathematical relationships would be more accurate. By increasing the number of shots fired from all angles below 90°, it is possible to apply Data Analytics and Machine Learning techniques for the incident angle determination process. It will be a complete study if it is possible to conduct a similar kind of analysis for different weapons and ammunition reported in various shooting incidents worldwide.

APPENDICES

Appendix A: Measured Lead-in Crease Length and Calculated Area of the Impact Mark

Table A1.   Measured Lead-in Crease Length of the Impact Mark and Incident Angle of Bullets

Incident angle	Number of processed data samples	Measured lead-in crease length (mm)										Average lead-in crease length (mm)
		Shot No. 1	Shot No. 2	Shot No. 3	Shot No. 4	Shot No. 5	Shot No. 6	Shot No. 7	Shot No. 8	Shot No. 9	Shot No. 10	
10º	5	27	26	27	28	27	No firing data					27
15º	10	22	18	15	19	19	19	17	20	20	21	19
20º	10	15	15	15	13	18	14	15	15	16	14	15
30º	10	9	10	8	9	9	8	9	10	9	9	9
40º	10	5	6	6	7	6	6	7	6	6	5	6

Table A2.   Calculated Area of the Impact Mark and Incident Angle of Bullets

Incident angle	Number of processed data samples	Calculated area of the impact mark (mm^2)										Average area (mm^2)
		Shot No. 1	Shot No. 2	Shot No. 3	Shot No. 4	Shot No. 5	Shot No. 6	Shot No. 7	Shot No. 8	Shot No. 9	Shot No. 10	
10º	5	657	638	610	738	702	No firing data					669
15º	10	276	241	230	302	297	253	231	241	270	289	263
20º	10	169	167	161	149	161	160	168	141	161	173	161
30º	10	106	104	95	107	103	92	94	96	96	97	99
40º	10	86	77	81	75	78	76	80	68	73	76	77
50º	10	65	64	74	68	63	65	66	61	70	74	67
60º	10	64	62	62	53	54	61	53	57	61	53	58
70º	10	58	60	55	57	56	50	51	52	51	50	54
80º	10	50	53	51	54	46	52	46	46	52	50	50
90º	10	49	53	48	50	46	47	52	49	46	50	49

Appendix B: Identified Mathematical Relationships using MATLAB

a. Mathematical Relationship of Incident Angle to the Average Lead-in Length of Bullet Impact Marks

General model Exp2:

$$f(x) = a * \exp(b * x) + c * \exp(d * x)$$

Coefficients (with 95% confidence bounds):

a =   1411   (-1.952e+05, 1.981e+05)

b =   -0.612   (-15.01, 13.79)

c =   38.35   (-3.583, 80.28)

d =   -0.04729 (-0.08861, -0.005982)

Goodness of fit:

SSE: 0.1359

R-square: 0.9995

Adjusted R-square: 0.998

RMSE: 0.3686

b. Mathematical Relationship of Average Lead-in Crease Length of Bullet Impact Marks to the Incident Angle

General model Exp2:

$$f(x) = a * \exp(b * x) + c * \exp(d * x)$$

Coefficients (with 95% confidence bounds):

a =   50.55   (-299.6, 400.7)

b =   -0.2892   (-2.602, 2.024)

c =   43.16   (-95.29, 181.6)

d =   -0.05481 (-0.1911, 0.08144)

Goodness of fit:

SSE: 0.3665

R-square: 0.9994

Adjusted R-square: 0.9975

RMSE: 0.6054

c.   Mathematical Relationship of Bullet Incident Angle to the Average Area of the Bullet Impact Marks

General model Exp2:

$$f(x) = a * \exp(b * x) + c * \exp(d * x)$$

Coefficients (with 95% confidence bounds):

$a =$ 6857   (4879, 8835)

$b =$ -0.2532   (-0.285, -0.2215)

$c =$ 141.1   (103.8, 178.4)

$d =$ -0.01356 (-0.01854, -0.008574)

Goodness of fit:

SSE: 268.9

R-square: 0.9992

Adjusted R-square: 0.9988

RMSE: 6.695

d.   Mathematical Relationship of the Average Area of the Bullet Impact Marks to the Incident Angle

General model Exp2:

$$f(x) = a * \exp(b * x) + c * \exp(d * x)$$

Coefficients (with 95% confidence bounds):

$a =$ 715.2   (106.7, 1324)

$b =$ -0.05052   (-0.06945, -0.03158)

$c =$ 27.51   (14.62, 40.39)

$d =$ -0.001756 (-0.003511, -1.809e-06)

Goodness of fit:

SSE: 55.53

R-square: 0.9922

Adjusted R-square: 0.9883

RMSE: 3.042

Appendix C: Computed Incident Angles for Evaluation Process

Table C1.   Computed Incident Angle Based on the Length of Bullet Lead-in Crease Mark

| Incident angle | Number of processed data samples | Computed incident angle | | | | | | | Average of the computed angles |
		Shot No. 1	Shot No. 2	Shot No. 3	Shot No. 4	Shot No. 5	Shot No. 6	Shot No. 7	
10º	7	10º	10º	9º	10º	9º	9º	11º	9.71º
20º	7	21º	21º	20º	20º	19º	19º	20º	20.00º
30º	7	34º	30º	31º	33º	29º	29º	30º	30.86º
40º	7	45º	43º	38º	39º	40º	40º	39º	40.57º

Table C2.   Computed Incident Angle Based on the Ellipse Method

| Incident angle | Number of processed data samples | Computed incident angle | | | | | | | Average of the computed angles |
		Shot No. 1	Shot No. 2	Shot No. 3	Shot No. 4	Shot No. 5	Shot No. 6	Shot No. 7	
10º	7	12.7	15.83	9.77	15.6	17.98	12.78	15.59	14.32º
20º	7	21.65	22.25	22.74	23.21	22.75	23.35	22.82	22.68º
30º	7	30.91	30.58	29.11	30.57	32.62	29.87	29.97	30.52º
40º	7	39.17	47.53	47.08	47.87	46.56	50.22	44.36	46.11º
50º	7	54.2	55.11	59.42	57.13	49.1	50.05	56.08	54.44º
60º	7	67.03	60.22	64.19	64.04	64.12	61.78	65.38	63.82º
70º	7	74.31	73.63	70.93	69.89	72.47	71.48	70.27	71.85º
80º	7	79.96	81.1	79.75	78.05	76.9	83.7	81.03	80.07º
90º	7	82.82	84.68	84.4	78.41	84.63	87.74	87.31	84.28º

Table C3.   Computed Incident Angle Based on the Full Impact Length Based Method

Incident angle	Number of processed data samples	Computed incident angle							Average of the computed angles
		Shot No. 1	Shot No. 2	Shot No. 3	Shot No. 4	Shot No. 5	Shot No. 6	Shot No. 7	
10º	7	4	3	4	4	3	4	3	3.5º
20º	7	19	19	20	22	19	20	19	19.7º
30º	7	33	30	32	29	31	32	32	31.2º
40º	7	40	43	43	43	44	43	41	42.4º
50º	7	51	52	47	51	48	52	51	50.3º
60º	7	57	56	60	56	62	63	60	59.1º
70º	7	69	69	72	70	71	70	71	70.2º
80º	7	80	79	86	76	80	81	74	79.4º
90º	7	88	90	85	90	88	90	83	87.7º

Table C4.   Computed Incident Angle Based on the Area of Bullet Impact Mark

Incident angle	Number of processed data samples	Computed incident angle							Average of the computed angles
		Shot No. 1	Shot No. 2	Shot No. 3	Shot No. 4	Shot No. 5	Shot No. 6	Shot No. 7	
10º	7	7º	5º	8º	9º	8º	12º	13º	8.86º
20º	7	21º	21º	21º	22º	21º	21º	21º	21.14º
30º	7	28º	26º	29º	26º	27º	32º	31º	28.43º
40º	7	36º	39º	38º	44º	38º	43º	38º	39.43º
50º	7	49º	51º	45º	47º	51º	51º	48º	48.86º
60º	7	64º	59º	57º	58º	66º	59º	69º	61.71º
70º	7	68º	66º	69 º	65º	67º	76 º	75º	69.43º
80º	7	82º	76º	82º	74º	87º	77º	88º	80.86º
90º	7	85º	86º	86º	90º	90º	88º	86º	87.29º

Appendix D: Calculating Root Mean Square Error for Data Evaluation Process

Table D1.   Root Mean Square Error calculated for all the computed angles under the Ellipse method, full impact length based method and impact area based approach

Actual incident angle	Ellipse method			Full impact length based method			Impact area based approach		
	Computed Average	Difference to the actual Incident angle	Squared value of the difference	Computed Average	Difference to the actual Incident angle	Squared value of the difference	Computed Average	Difference to the actual Incident angle	Squared value of the difference
10º	14.32	4.32	18.6624	3.5	-6.5	42.25	8.86	-1.14	1.2996
20º	22.68	2.68	7.1824	19.71	-0.29	0.0841	21.14	1.14	1.2996
30º	30.52	0.52	0.2704	31.2	1.2	1.44	28.43	-1.57	2.4649
40º	46.11	6.11	37.3321	42.4	2.4	5.76	39.43	-0.57	0.3249
50º	54.44	4.44	19.7136	50.3	0.3	0.09	48.86	-1.14	1.2996
60º	63.82	3.82	14.5924	59.1	-0.9	0.81	61.71	1.71	2.9241
70º	71.85	1.85	3.4225	70.2	0.2	0.04	69.43	-0.57	0.3249
80º	80.07	0.07	0.0049	79.4	-0.6	0.36	80.86	0.86	0.7396
90º	84.28	-5.72	32.7184	87.78	-2.22	4.9284	87.29	-2.71	7.3441
Average of the squared difference		14.87768			6.19583				2.00236
RMSE value		**3.857159**			**2.48914**				**1.41505**

REFERENCES

[1].   7.62   x   39   mm   [WWW   Document],   2022.   .   Wikipedia.   URL https://en.wikipedia.org/w/index.php?title=7.62%C3%9739mm&oldid=1075877849 (accessed 4.2.22).

[2].   ABFO No. 2 Photomacrographic Scale [WWW Document], 2022. . Forensics Source. URL   https://forensicssource.com/products/abfo-no-2-photomacrographic-scale   (accessed 11.9.22).

[3].   CvInvoke.ContourArea   Method   [WWW   Document],   2020.   URL https://www.emgu.com/wiki/files/4.5.1/document/html/6ef05086-8aa7-3f1b-a27f-42594e776465.htm (accessed 11.9.22).

[4].   CvInvoke.DrawContours   Method   [WWW   Document],   2020.   URL https://www.emgu.com/wiki/files/4.5.1/document/html/3609fbca-96a2-ebdb-102f-668b62b9718e.htm (accessed 11.9.22).

[5].   CvInvoke.FindContours   Method   [WWW   Document],   2019.   URL https://www.emgu.com/wiki/files/4.1.0/document/html/cb24a129-d9ce-57f3-19ad-0eaa27a77317.htm (accessed 11.9.22).

[6].   Divinext Digital Inclinometer Electronic Protractor [WWW Document], 2022. . Flipkart.com.   URL   https://www.flipkart.com/divinext-digital-inclinometer-electronic-protractor-aluminum-alloy-shell-bevel-box-angle-finder-gauge-meter-precision-measurements-base-spirit-level-magnetic/p/itmffh5pcbhhavpn (accessed 4.23.22).

[7].   DSLR | EOS   90D | Canon   USA   [WWW   Document],   2020.   URL https://www.usa.canon.com/internet/portal/us/home/products/details/cameras/eos-dslr-and-mirrorless-cameras/dslr/eos-90d-body (accessed 4.6.22).

[8].   Emgu CV: OpenCV in .NET (C#, VB, C++ and more) [WWW Document], 2022. URL https://www.emgu.com/wiki/index.php/Main_Page (accessed 4.6.22).

[9].   Forensic Rulers and Scales: Types, Characteristics, and Uses [WWW Document], 2021.   .   Forensic   Reader.   URL   https://forensicreader.com/rulers-and-scales-types-uses/ (accessed 4.6.22).

[10].   Forensic Science - Shooting Scene Reconstruction [WWW Document], 2022. URL https://dps.mn.gov/divisions/bca/bca-divisions/forensic-science/Pages/forensic-programs-crime-scene-ssrecon.aspx (accessed 3.28.22).

[11].   Forensic   science   [WWW   Document],   2022.   .   Wikipedia.   URL https://en.wikipedia.org/w/index.php?title=Forensic_science&oldid=1119483344   (accessed 11.7.22).

[12].   Gonzalez, R.C., Woods, R.E., 2008. Digital image processing, 3rd ed. ed. Prentice Hall, Upper Saddle River, N.J.

[13].   GrabCut for Automatic Image Segmentation [OpenCV Tutorial] [WWW Document], 2022. URL https://www.sicara.fr/blog-technique/grabcut-for-automatic-image-segmentation-opencv-tutorial (accessed 11.8.22).

[14]. GrabCut [WWW Document], 2021. . Wikipedia. URL https://en.wikipedia.org/w/index.php?title=GrabCut&oldid=1014501536 (accessed 11.8.22).

[15]. Graphics.SmoothingMode Property (System.Drawing) [WWW Document], 2022. URL https://learn.microsoft.com/en-us/dotnet/api/system.drawing.graphics.smoothingmode?view=windowsdesktop-7.0 (accessed 11.9.22).

[16]. Haag, M.G., Haag, L.C., 2011. Shooting incident reconstruction, Second edition. ed. Academic Press, Burlington, MA.

[17]. Hueske, E.E., 2016. Practical analysis and reconstruction of shooting incidents, Second edition. ed. CRC Press.

[18]. Image(TColor, TDepth).Dilate Method [WWW Document], 2015. URL https://emgu.com/wiki/files/3.0.0/document/html/28088b77-7d94-d1a7-9793-8dcec6b70ac5.htm (accessed 11.9.22).

[19]. Image(TColor, TDepth).Erode Method [WWW Document], 2015. URL https://emgu.com/wiki/files/3.0.0/document/html/9d6ac86b-0c0f-97f1-79a6-4eb7dc0a0d6d.htm (accessed 11.9.22).

[20]. Image(TColor, TDepth).GrabCut Method [WWW Document], 2020. URL https://www.emgu.com/wiki/files/4.5.1/document/html/42b92565-8dd7-b78d-6b23-71f246d88ef2.htm (accessed 11.9.22).

[21]. Image(TColor, TDepth).SmoothMedian Method [WWW Document], 2015. URL https://emgu.com/wiki/files/3.0.0/document/html/c1760a7d-a3c8-ccb0-0884-e4e10bf9e71f.htm (accessed 11.9.22).

[22]. Image(TColor, TDepth).Sub Method (Image(TColor, TDepth), Image(Gray, Byte)) [WWW Document], 2020. URL https://www.emgu.com/wiki/files/4.5.1/document/html/373d6261-304e-31e3-5e19-2c6fbefdec75.htm (accessed 9.12.22).

[23]. Image(TColor, TDepth).ThresholdBinary Method [WWW Document], 2020. URL https://www.emgu.com/wiki/files/4.5.1/document/html/046038a6-4e0e-ba4c-d01f-eb3fc1c29383.htm (accessed 5.20.22).

[24]. Labradar: The new generation of ballistic velocity radar | Labradar, 2017. URL https://mylabradar.com/ (accessed 4.23.22).

[25]. MATLAB - MathWorks [WWW Document], 2022. URL https://www.mathworks.com/products/matlab.html (accessed 11.12.22).

[26]. Morphology - Closing [WWW Document], 2003. URL https://homepages.inf.ed.ac.uk/rbf/HIPR2/close.htm (accessed 11.9.22).

[27]. .NET Framework 4.5 [WWW Document], 2022. . Microsoft Download Center. URL https://www.microsoft.com/en-us/download/details.aspx?id=30653 (accessed 4.6.22).

[28]. Nishshanka, B., Shepherd, C., Ariyarathna, R., 2021. AK bullet (7.62 × 39 mm) holes on 1-mm sheet metal: A forensic-related study in aid of bullet trajectory reconstruction. J Forensic Sci 66, 1276–1284. https://doi.org/10.1111/1556-4029.14717

[29]. Nishshanka, B., Shepherd, C., Ariyarathna, R., 2020a. A software based solution to estimate the angles of incidence of AK bullets using bullet hole features on 1mm sheet metal.

[30]. Nishshanka, B., Shepherd, C., Paranirubasingam, P., 2020b. Forensic based empirical study on ricochet behaviour of Kalashnikov bullets (7.62 mm × 39 mm) on 1 mm sheet metal. Forensic Science International 312, 110313. https://doi.org/10.1016/j.forsciint.2020.110313

[31]. Nishshanka, L.C.B., Shepherd, C., Ariyarathna, M.R., Weerakkody, L., Palihena, J., 2021. An android-based field investigation tool to estimate the potential trajectories of perforated AK bullets in 1 mm sheet metal surfaces. Forensic Science International: Digital Investigation 38, 301267. https://doi.org/10.1016/j.fsidi.2021.301267

[32]. OpenCV [WWW Document], 2022. . OpenCV. URL https://opencv.org/ (accessed 5.6.22).

[33]. Pythagoras Theorem (Pythagorean) - Formula, Proof, Examples [WWW Document], 2021. . Cuemath. URL https://www.cuemath.com/geometry/pythagoras-theorem/ (accessed 11.9.22).

[34]. RMSE: Root Mean Square Error [WWW Document], 2022. . Statistics How To. URL https://www.statisticshowto.com/probability-and-statistics/regression-analysis/rmse-root-mean-square-error/ (accessed 11.20.22).

[35]. Salt-and-pepper noise [WWW Document], 2022. . Wikipedia. URL https://en.wikipedia.org/w/index.php?title=Salt-and-pepper_noise&oldid=1085283109 (accessed 11.8.22).

[36]. STABILA Type 196-2 K Mason Levels [WWW Document], 2022. URL https://www.stabila.com/en-US/products-553/details/type-196-2-k-mason-levels.html (accessed 10.19.22).

[37]. The 6 Reasons You Should Convert RGB to Grayscale in Image Editing – C4RE.GR [WWW Document], 2022. URL https://c4re.gr/rgb-to-grayscale-conversion/ (accessed 9.12.22).

[38]. Type 56 Assault Rifle [WWW Document], 2022. . Wikipedia. URL https://en.wikipedia.org/w/index.php?title=Type_56_assault_rifle&oldid=1081545180 (accessed 4.2.22).

[39]. Types of Morphological Operations - MATLAB & Simulink [WWW Document], 2022. URL https://www.mathworks.com/help/images/morphological-dilation-and-erosion.html (accessed 11.9.22).

[40]. Visual Studio: IDE and Code Editor for Software Developers and Teams [WWW Document], 2022. . Visual Studio. URL https://visualstudio.microsoft.com (accessed 4.6.22).

[41].   Walters, M., Liscio, E., 2020. The Accuracy and Repeatability of Reconstructing Single Bullet Impacts Using the 2D Ellipse Method. J Forensic Sci 65, 1120–1127. https://doi.org/10.1111/1556-4029.14309

[42].   Why did the AK-47 become so popular? [WWW Document], 2016. . The Economist. URL   https://www.economist.com/the-economist-explains/2014/01/08/why-did-the-ak-47-become-so-popular (accessed 3.28.22).